A TIME DOMAIN SIMULATION

OF A

BEAM CONTROL SYSTEM

(12)

eirs
ENGINEERING & INDUSTRIAL RESEARCH STATION
ELECTRICAL ENGINEERING

Prepared for

AIR FORCE OFFICE OF SCIENTIFIC RESEARCH

BOLLING AFB, D.C.

By

Jerrel R. Mitchell, Ph.D.

Mississippi State University
Mississippi State, MS 39762

MSSU-EIRS-EE-81-3

COLLEGE OF ENGINEERING ADMINISTRATION

WILLIE L. MCDANIEL, PH.D.
DEAN, COLLEGE OF ENGINEERING

WALTER R. CARNES, PH.D
ASSOCIATE DEAN

JOHN I. PAULK, PH.D.
ASSOCIATE DEAN

LAWRENCE J. HILL, M.S.
DIRECTOR, ENGINEERING SERVICES

CHARLES B. CLIETT, M.S.
AEROSPACE ENGINEERING

WILLIAM R. FOX, PH.D.
AGRICULTURAL & BIOLOGICAL ENGINEERING

JOHN L. WEEKS, JR., PH.D.
CHEMICAL ENGINEERING

ROBERT M. SCHOLTES, PH.D.
CIVIL ENGINEERING

B. J. BALL, PH.D.
ELECTRICAL ENGINEERING

W. H. EUBANKS, M.ED.
ENGINEERING GRAPHICS

FRANK E. COTTON, JR., PH.D.
INDUSTRIAL ENGINEERING

C. T. CARLEY, PH.D.
MECHANICAL & NUCLEAR ENGINEERING

ELDRED W. HOUGH, PH.D.
PETROLEUM ENGINEERING

For additional copies or information
address correspondence to

ENGINEERING AND INDUSTRIAL RESEARCH STATION
DRAWER DE
MISSISSIPPI STATE UNIVERSITY
MISSISSIPPI STATE, MISSISSIPPI 39762

TELEPHONE (601) 325-2266

UNCLASSIFIED

SECURITY CLASSIFICATION OF THIS PAGE (When Data Entered)

REPORT DOCUMENTATION PAGE	READ INSTRUCTIONS BEFORE COMPLETING FORM
1. REPORT NUMBER: AFOSR-TR-81-0323	2. GOVT ACCESSION NO.: AD-A097 423
	3. RECIPIENT'S CATALOG NUMBER: 9
4. TITLE (and Subtitle): A TIME DOMAIN SIMULATION OF A BEAM CONTROL SYSTEM	5. TYPE OF REPORT & PERIOD COVERED: FINAL 1 Jan [redacted] - 31 Dec [redacted]
	6. PERFORMING ORG. REPORT NUMBER
7. AUTHOR(s): Jerrel R. Mitchell, Ph.D.	8. CONTRACT OR GRANT NUMBER(s): AFOSR-80-0108
9. PERFORMING ORGANIZATION NAME AND ADDRESS: Mississippi State University, Drawer EE, Mississippi State, MS 39762	10. PROGRAM ELEMENT, PROJECT, TASK AREA & WORK UNIT NUMBERS: 2305/09, 61102F
11. CONTROLLING OFFICE NAME AND ADDRESS: Air Force Office of Scientific Research, AFOSR/NE, Building 410, Bolling AFB, D.C. 20332	12. REPORT DATE: Feb [redacted] 81
	13. NUMBER OF PAGES: 44
14. MONITORING AGENCY NAME & ADDRESS (if different from Controlling Office)	15. SECURITY CLASS. (of this report): UNCLASSIFIED
	15a. DECLASSIFICATION/DOWNGRADING SCHEDULE

16. DISTRIBUTION STATEMENT (of this Report)

Approved for public release;
distribution unlimited.

17. DISTRIBUTION STATEMENT (of the abstract entered in Block 20, if different from Report)

19. KEY WORDS (Continue on reverse side if necessary and identify by block number)

Time Domain Simulation, Beam Control Systems, MIMIC Simulation

20. ABSTRACT (Continue on reverse side if necessary and identify by block number)

The Airborne Laser Laboratory (ALL) is being developed by the Air Force to investigate the integration and operation of high energy laser components in dynamic airborne environment and to study the propagation of laser light from an airborne vehicle to an airborne target. The ALL is composed of several systems; among these are the Airborne Pointing and Tracking System (APT) and the Automatic Alignment System (AAS). This report presents the results of performing a time domain dynamic simulation for an integrated beam

DD FORM 1 JAN 73 1473

UNCLASSIFIED

SECURITY CLASSIFICATION OF THIS PAGE (When Data Entered)

control system composed of the APT and AAS.

The simulation is performed on a digital computer using the MIMIC language. It includes models of the dynamics of the system and of disturbances. Also presented in the report are the rationales and developments of these models.

The data from the simulation code is summarized by several plots. In addition results from massaging the data with waveform analysis packages are presented. The results are discussed and conclusions are drawn.

AFOSR-TR- 81-0323

A TIME DOMAIN SIMULATION OF A BEAM CONTROL SYSTEM

BY

Jerrel R. Mitchell, Ph.D.

Final Report

Grant No. AFOSR-80-0108

For

Period of January 1, 1980 - December 31, 1980

Department of Electrical Engineering
Mississippi State University
Mississippi State, MS 39762

February 28, 1981

ABSTRACT

The Airborne Laser Laboratory (ALL) is being developed by the Air Force to investigate the integration and operation of high energy laser components in dynamic airborne environment and to study the propagation of laser light from an airborne vehicle to an airborne target. The ALL is composed of several systems; among these are the Airborne Pointing and Tracking System (APT) and the Automatic Alignment System (AAS). This report presents the results of performing a time domain dynamic simulation for an integrated beam control system composed of the APT and AAS.

The simulation is performed on a digital computer using the MIMIC language. It includes models of the dynamics of the system and of disturbances. Also presented in the report are the rationales and developments of these models.

The data from the simulation code is summarized by several plots. In addition results from massaging the data with waveform analysis packages are presented. The results are discussed and conclusions are drawn.

TABLE OF CONTENTS

LIST OF FIGURES

LIST OF TABLES

LIST OF SYMBOLS AND ABBREVIATIONS

AAS	-	Automatic Alignment System
ALL	-	Airborne Laser Laboratory
APT	-	Automatic Pointing and Tracking System
BANG	-	MIMIC Variable for Beam Angle
BMD	-	Base Motion Distrubance and MIMIC Variable for BMD Signal
[ ]	-	Denotes a Reference
EAAS	-	MIMIC Variable for AAS Error Signal
ESTAB	-	MIMIC Variable for Stabilized Platform Error Signal
IMC	-	Image Motion Compensation
LOS	-	Line of Sight
PSD	-	Power Spectrical Density
RMS	-	Root Mean Square
S/H	-	Sample-Hold Process
SIGNAL	-	MIMIC Variable for Target Signal
STAB ERROR	-	Error Signal of Stabilized Platform (Corresponds to MIMIC Variable ESTAB)
θ_{BMD}	-	Base Motion Distrubance Signal
θ_S	-	Target Signal
$\dot{\theta}_S$	-	First Derivative w.r.t. t of θ_S
$\ddot{\theta}$	-	Second Derivative w.r.t. t of θ_S

LIST OF SYMBOLS AND ABBREVIATIONS

(Continued)

θ_T	-	Tracker Noise Signal
θ_B	-	Beam Angle
θ_G	-	Gimbal Angle
T	-	Sampling Period
TRKERR	-	MIMIC Variable for Tracker Noise
TRACKER ERROR	-	Error Signal from Tracker (Corresponds to MIMIC Variable X1)
w.r.t.	-	With Respect To

I. INTRODUCTION

The Airborne Laser Laboratory is composed of several systems. Among these are the Airborne Pointing and Tracking System (APT) and the Automatic Alignment System (AAS). The primary functions of the APT are (1) performance of precision tracking and (2) stabilization of the optical line of sight (LOS) to the target. The primary function of the AAS is to compensate for static misalignments of the laser beam; a secondary function is to aid the APT in the stability of the LOS. Two causes of instability of the LOS are base motion disturbance (BMD) and target motion. In order to reduce the effects of BMD on the stability of the beam LOS studies were initiated to determine the feasibility of using the Automatic Alignment System in conjunction with the APT, for beam control. (Ref. 1, 2).

The scheme devised for reducing BMD involves feeding the stab gyro output through a 100 Hz low pass filter; then to the AAS and to the image motion compensation (IMC) input of the tracker. (See Figure 1). The 100 Hz low pass filter minimizes errors due to high frequency gyro resonances. Feeding the gyro output through the 100 Hz filter to the image motion compensation and to the AAS produces a transfer function between the BMD input, θ_{BMD}, and the beam angle, θ_B, that is approximately zero for frequencies below 100 Hz. For frequencies significantly greater than 100 Hz the affect on θ_B by θ_{BMD} is practically unaltered by the feedforward

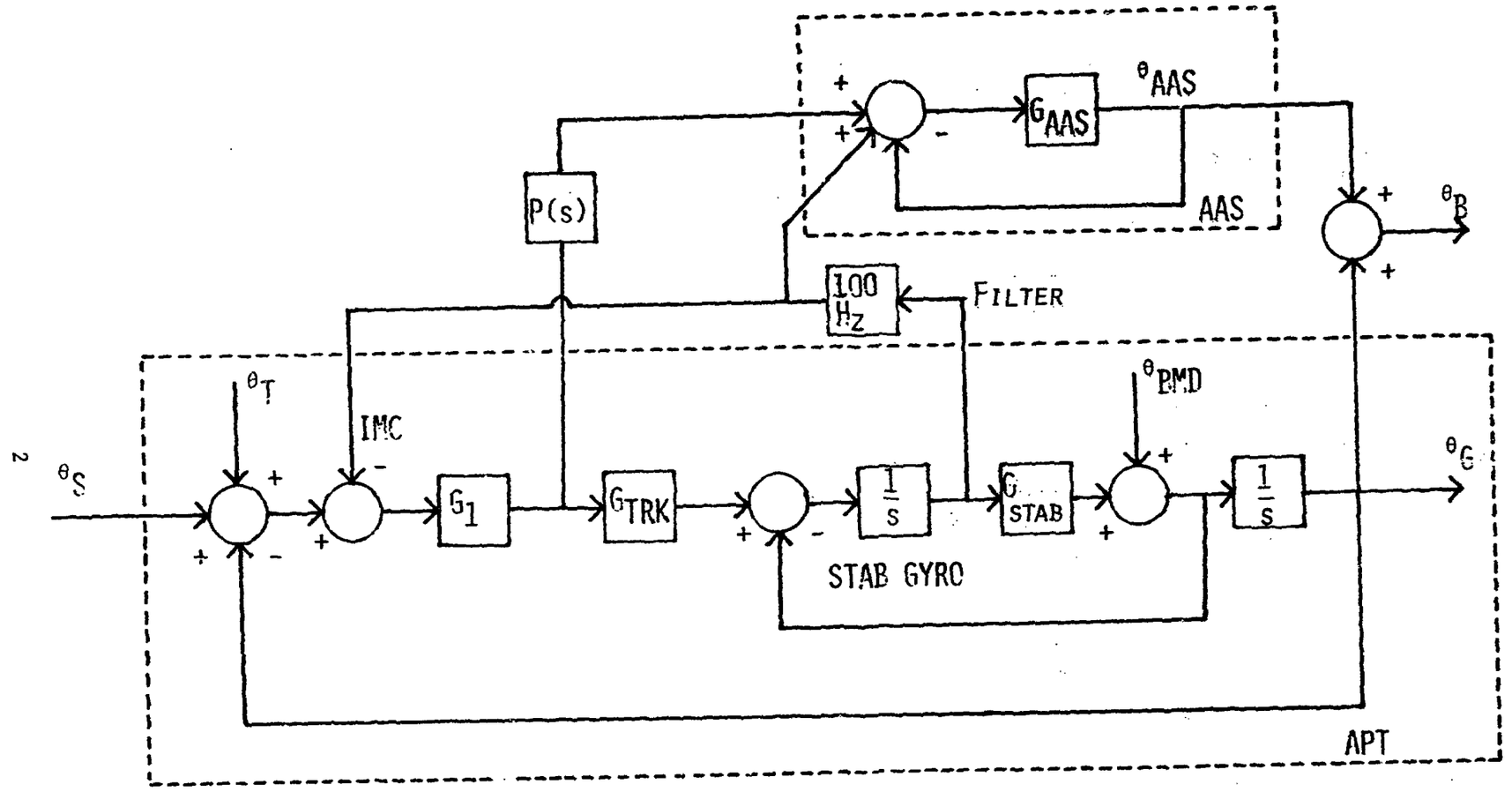

FIGURE 1. FEED FORWARD SCHEME FOR BEAM CONTROL

scheme. Fortunately most of the energy of θ_{BMD} occurs in the frequency range below 100 Hz. Furthermore, the pure integration between θ_{BMD} and θ_B will greatly reduce the effects on the beam angle of signal components in the greater than 100 Hz range.

The above scheme is shown in [2] to greatly improve BMD rejection but does not improve the capability of the system to track targets with significant motion relative to the APT/AAS. In order to provide this capability it was decided to feed the tracker error to the input of the AAS. This results in an overall increase in the bandwidth of the system by a factor of twenty. The major disadvantage of this scheme is that the effect on θ_B due to tracker noise θ_T is amplified.

The tracker noise and the target signal θ_S are modeled as entering at the same point. (See Figure 1). Thus, the combined beam control system (APT/AAS) has the same filtering affect on both signals. Fortunately the power density spectrums (PSD's) of θ_S and θ_T differ. Typically for a "flyby" target the PSD of θ_S is low frequency dominated where the PSD for θ_T is approximately flat up to 30 Hz. The transfer function P(s) in Figure 1 is inserted to provide compromise filtering between θ_B and θ_T so as to reduce the beam error, $(\theta_S - \theta_B)$.

In an ideal system the transfer function between θ_B and θ_S should be unity. However, because of the system dynamics a unity transfer function is impossible. The beam angle is a function of θ_S, θ_T, and θ_{BMD}; consequently, the beam error is also a function of these. For the system to perform high precision

tracking, the beam error must be small. In the frequency domain this corresponds to requiring the PSD of the beam error to be as small as possible over the frequency spectrum.

The design criterion for the filter then is the P(s) that minimizes the root mean square (RMS) of the beam error. In [3] a computer code for performing this minimization is presented. This code was used to design optimal P(s)'s for several cases of "flyby" type scenarios. (See Figure 2). The results are summarized in Table I. Data is presented for comparing the no feed forward to the feed forward with P=1 case and the optimal P's cases and for comparing the P=1 to the optimal P's cases. The P=1 case is presented since this is the logical choice for P without optimization. In addition improvements of the optimal P's to the P=1 cases are presented. This table shows that simple optimal lead-lag type filters in the feed forward scheme can produce marked reductions in the RMS beam errors.

The results obtained in [3] show the feasibility of controlling the beam angle with a high degree of accuracy. However the figures of merit are based on RMS values of error. RMS errors do not provide any information concerning the dynamics of the errors, e.g., maximum and minimum values and the points in time of occurance. In addition, in the study in [3] the sampling effects of the tracker were ignored. Thus, in order to validate the results obtained in [3], a time domain simulation of the feed forward scheme is presented in this report.

Y_o (M)	PERCENT IMPROVEMENTS			CLOSED LOOP BW(hz)	DESCRIPTION OF OPTIMAL P_2				
	$P_2 = 1$ TO NO FEEDFORWARD	OPTIMAL P_2 TO NO FEEDFORWARD	OPTIMAL P_2 TO $P_2 = 1$		D.C. GAIN	BREAK FREQUENCIES FOR ZEROS		BREAK FREQUENCIES FOR POLES	
500	98.5	99.0	34.2	29.4	.9973	1.349	16.01	1.524	12.68
1000	97.8	97.9	7.0	23.9	.9986	1.631	25.04	1.941	9.829
2000	95.5	96.0	10.7	19.9	.9979	1.142	23.34	1.282	6.311
5000	90.5	91.9	14.5	18.3	.9986	.9242	13.8	.9596	4.815

TABLE 1. RESULTS FROM EXECUTION OF THE OPTIMIZATION CODE

The simulation is implemented in the MIMIC Language. (Ref. 4). The development process for the simulation involves developing models of the signals and the blocks of Figure 1. These developments are presented in the two sections that follow. Following these is the results from executing the simulation code, along with analyses of the results and conclusions.

II. SIGNAL MODELS

Figure 1 shows three sources of external signals entering the APT/AAS pointing system. These are the target signal θ_S, the tracker error θ_T and the base motion disturbance θ_{BMD}. In [3] PSD's of each of these were used; however, here time domain representations of these signals are needed. These time domain models are developed in the following.

A. TARGET SIGNAL MODEL

A "flyby" type scenario as shown in Figure 2 is assumed for the target signal. The equation that describe the angle of the target w.r.t. the APT/AAS is

$$\theta_S = \tan^{-1} \frac{x}{Y_0} \tag{1}$$

where

$$x = x_0 + vt \ . \tag{2}$$

In (1) and (2) Y_0 is the minimum approach of the target to the APT/AAS pointing system, v is velocity (assumed to be constant), t is time, and x_0 is the initial x value where tracking is to be initiated. Tracking is assumed to begin two seconds before the target reaches its closest approach to the APT/AAS and continues for four seconds afterward. Therefore, the tracking duration is always four seconds, but the point where tracking starts depends upon v and Y_0.

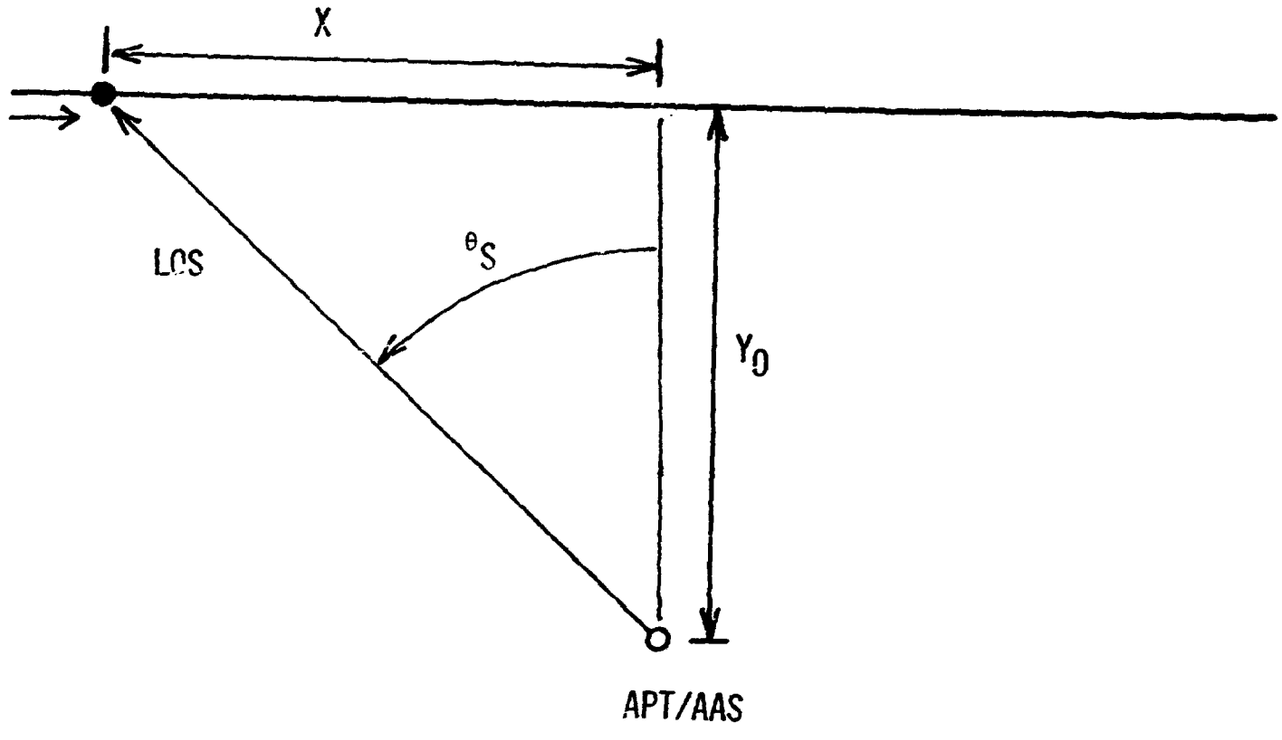

FIGURE 2. FLY-BY TYPE SCENARIO

In order to minimize transient effects due to the initiation of tracking it is assumed that an automatic handoff system will exist, i.e, the initiation of tracking will be smooth. Without the automatic handoff the derivative of the target signal appears as typified in Figure 3(a). At the times where tracking starts T_0 and ends T_F the derivative changes discontinuously. The discontinuity at T_0 causes transient effects that can be detrimental to good tracking performance. When tracking starts it is best that the beam angle be positioned, moving and accelerating the same as the LOS to the target. An automatic handoff system will provide these initial conditions. In order to simulate the automatic handoff system a fourth order polynomial spline is attached to the target signal (thus, generating a fictitious target signal for time less than T_0). The requirements on the spline are

$$\dot{\theta}'(T_0-4) = 0$$
$$\ddot{\theta}'(T_0-4) = 0$$
$$\theta'(T_0) = \theta(4)$$
$$\dot{\theta}'(T_0) = \dot{\theta}'(4)$$
$$\ddot{\theta}'(T_0) = \ddot{\theta}(4)$$

For simplicity in the following it is assumed that $T_0-4 = 0$. In essense the target signal will be "faked" by the spline for

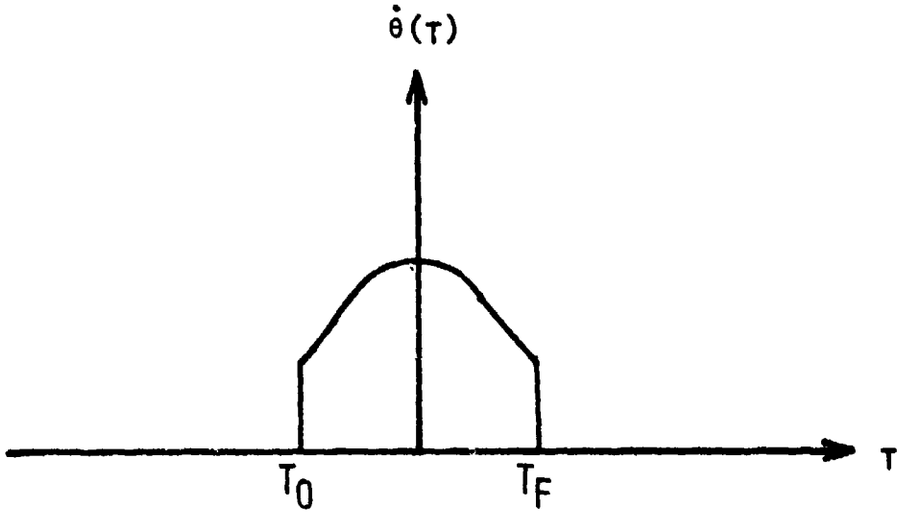

(A) TYPICAL SIGNAL RATE

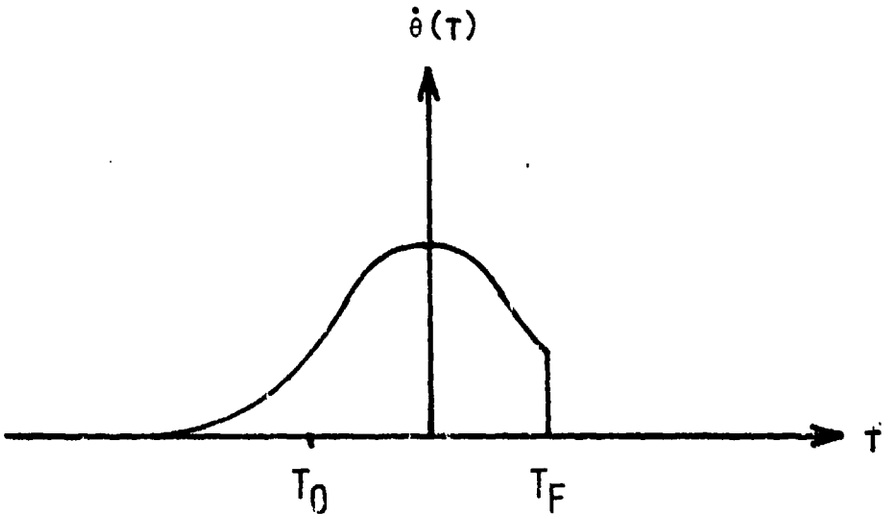

(B) TARGET SIGNAL RATE WITH SPLINE ON LEFT

FIGURE 3: TYPICAL TARGET SIGNAL ANGULAR VELOCITY

$0 \leq t \leq 4$ seconds and from $4 \leq t \leq 6$ tracking of the target will occur*. The impact on the derivative of the target signal by the spline is illustrated in Figure 3(b).

B. TRACKER NOISE MODEL

In [2] the tracker noise is approximated as having a flat PSD up to 30 Hz and having an RMS value of 3.1 rad. In actuality the tracker noise is a train of uniformly occurring random pulses, e.g., see Figure 4. The amplitude of each pulse is assumed to be normally distributed with zero mean and a variance of σ^2. The power spectral density of a waveform of this type is

$$\phi(\omega) = \sigma^2 T \frac{\sin^2(\omega T/2)}{(\omega T/2)^2} \tag{3}$$

where T (sampling period) is the duration of each pulse. For the tracker being considered in this study $\sigma^2 = 9.61 \times 10^{-12}$ and $T = 0.01666$s.

A plot of the power spectrum density of the model used in this study is shown in Figure 5. The PSD is approximately flat up to 30 Hz as specified above. Thus, for generating this signal in the MIMIC code all that is required is to sample and hold every T seconds a normally distributed waveform with zero mean and a variance of σ^2.

---

* The discontinuity at the end of tracking T_F is not considered detrimental since it occurs after tracking has ceased.

C. BASE MOTION DISTURBANCE MODEL

In [1], [2], and [3] an experimental PSD for BMD was utilized. In order to generate a time domain signal with the characteristics of the experimental PSD, a normally distributed train of pulses with zero mean and variance of σ^2 is generated and filtered to obtain the desired PSD characteristics. The PSD of such a waveform is

$$\Phi_{BMD}(\omega) = \sigma^2 T \frac{\sin^2(\omega T/2)}{(\omega T/2)^2} |G(j\omega)|^2 \tag{4}$$

where T is the pulse durations and $G(j\omega)$ is the filter. By trial and error the filter that produces a PSD approximately equal to that of the previous studies is

$$G(j\omega) = \frac{\left(\frac{j\omega}{9} + 1\right)}{j\omega\left(\frac{j\omega}{200} + 1\right)} \tag{5}$$

when $T = 0.00628319$ and $\sigma^2 = 1.4324 \times 10^{-4}$. A plot of the PSD is shown in Figure 6. Circles on Figure 6 indicate points from the experimental PSD used in [3]. A close correlation between the data is seen.

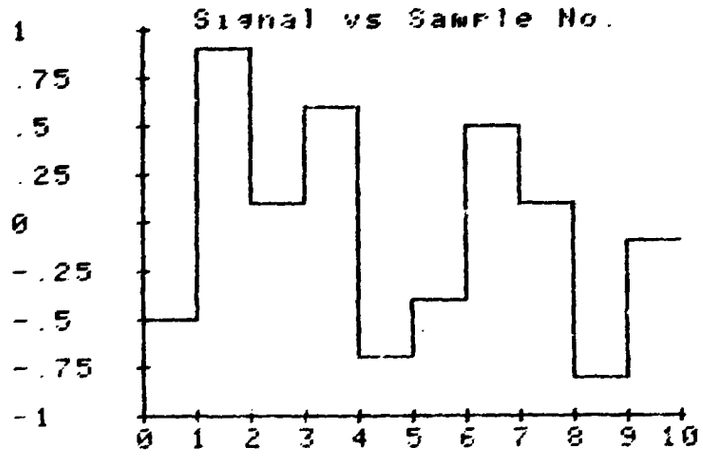

FIGURE 4. TYPICAL TRACKER NOISE

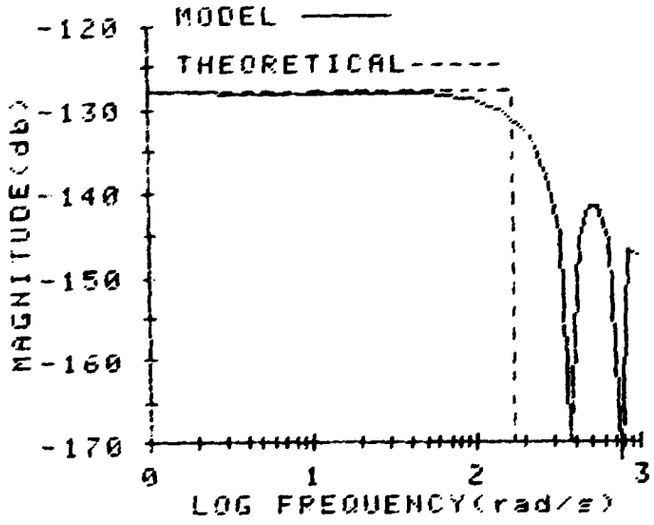

FIGURE 5. PSD'S OF TRACKER NOISE

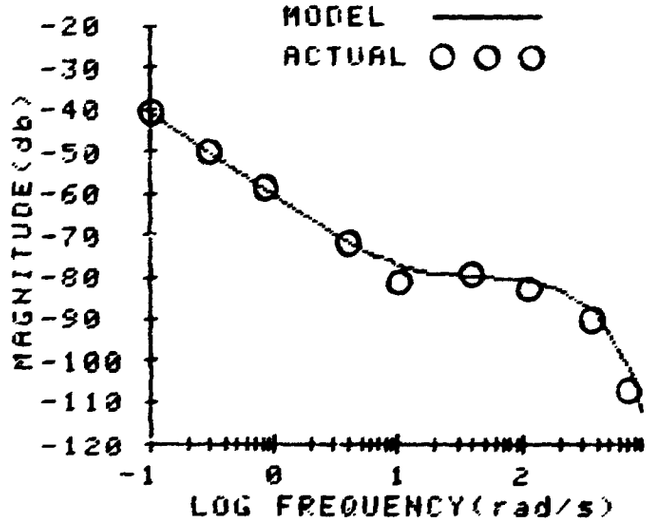

FIGURE 6. PSD'S OF BMD

III. DEVELOPMENT OF THE MIMIC SIMULATION

In order to expedite the development of the MIMIC simulation, Figure 1 is redrawn in a more general form in Figure 7. On this figure MIMIC variable assignments have been made, e.g., tracker error is denoted as TRKERR and base motion disturbance is BMD. The transfer functions used in the development of the MIMIC simulation are as follows:

$$G_1(s) = e^{-0.003s} \tag{6}$$

$$G_2(s) = \frac{33.02s+350}{s} \tag{7}$$

$$G_3(s) = \frac{1}{s} \tag{8}$$

$$G_4(s) = \frac{265.3s + 10^4}{1.274\times10^{-8}s^4+3.568\times10^{-6}s^3+4.715\times10^{-3}s^2+s} \tag{9}$$

$$G_5(s) = \frac{1}{s} \tag{10}$$

$$G_6(s) = \frac{1987s+1.248\times10^6}{s^2} \tag{11}$$

$$H_1(s) = \frac{1.0}{1.592\times10^{-3}s+1.0} \tag{12}$$

P(s) depends on the case being considered, i.e, either zero for no feed forward, unity, or anyone of the optimal P(s)'s from Table I. In addition for the no feed forward and stab not fed forward cases the 100 Hz filter is set to zero.

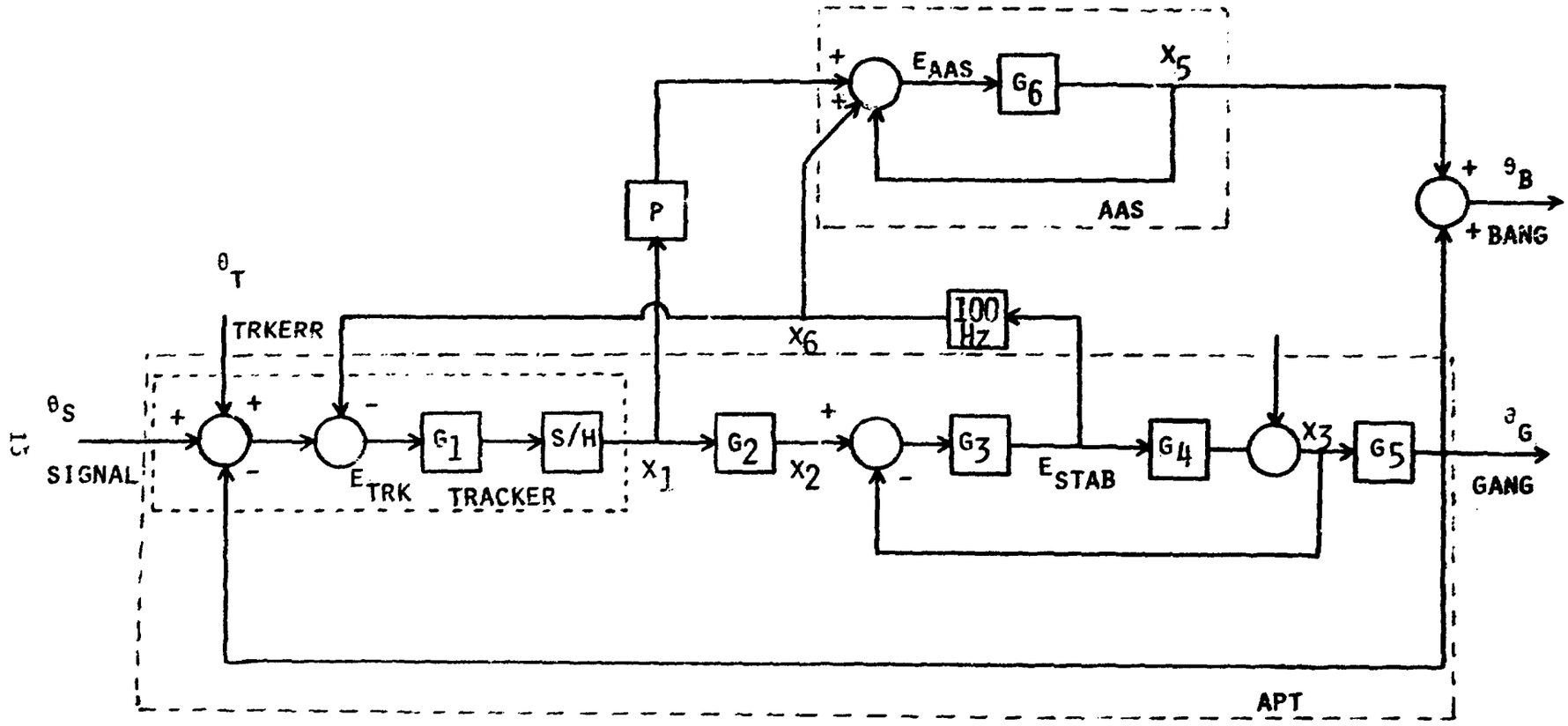

FIGURE 7. GENERALIZED BLOCK DIAGRAM OF APT/AAS FOR BEAM CONTROL

It should be noted that $G_1(s)$ is different from that used in [3]. In this previous study $G_1(s)$ is modeled as a three millisecond delay in cascade with the transfer function of a zero order hold. This is an approximation. In actuality the tracker involves a sampling process. In order for the MIMIC simulation to be a more accurate representation of the actual system the equivalence in this report of $G_1(s)$ is a 3 millisecond delay, whose transfer function is (6), in cascade with a sample and hold, i.e. the cascade combination of $G_1(s)$ and the block labeled S/H in Figure 7.

Using Figure 7, converting each transfer function to a corresponding set of differential/algebraic equations, and using the signal models of the preceding sections the MIMIC code presented in the Appendix was developed for simulating the APT/AAS beam control system. The code has been commented for ease in following.

IV. SIMULATION RESULTS

The code used in Appendix A is used to simulate the APT/AAS beam control system for four cases of the flyby type scenario, in particular, Y_0 = 500m, 1000m, 2000m, and 5000m. In addition five different beam control configurations are simulated: (1) no feed forward (2) tracker error not fed forward, (3) stab error not fed forward, (4) complete feed forward with P(s) = 1, (5) and complete feed forward with the optimal P(s). In the second configuration the stab error is still fed to the AAS and fed back to the IMC. In the third configuration the path from the stab error to the AAS and IMC are severed and the optimal P(s) is used in the tracker error to AAS path.

Target signals of the four cases of the flyby type scenario are shown in Figure 8. The plots include the spline signals (0 to 4 seconds) plus the assumed target signals (4 to 8 secondsl). As expected the closer the target comes to the APT/AAS the greater the angular velocity and acceleration of the target with respect to the APT/AAS.

Results from the simulation for determining the performance of the five configurations and for the four cases of the flyby scenario are shown in Figure 9-13. Tracker noise and base motion disturbances are included in all simulations. Each figure shows

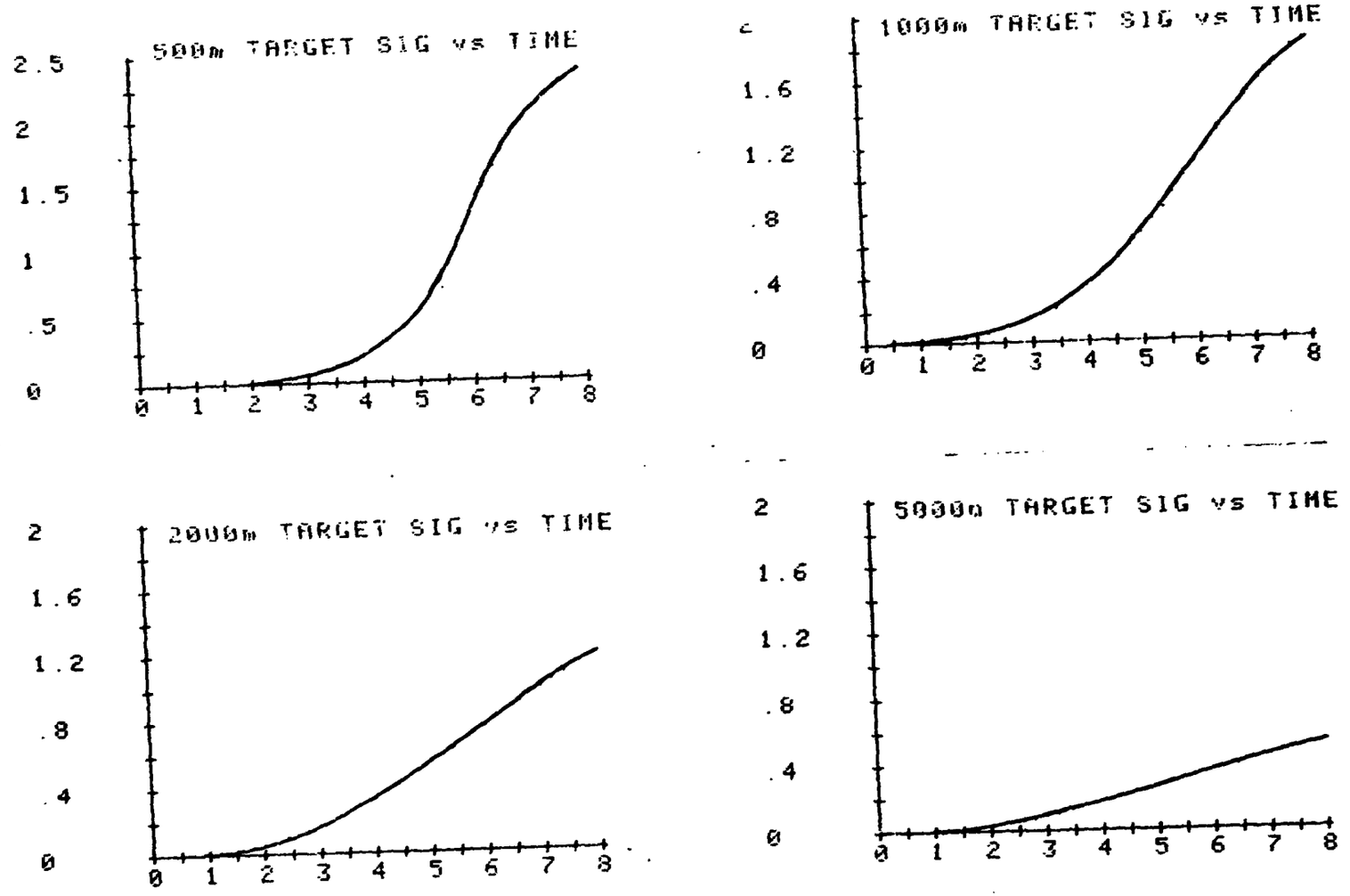

FIGURE 8. TARGET SIGNALS USED IN SIMULATION

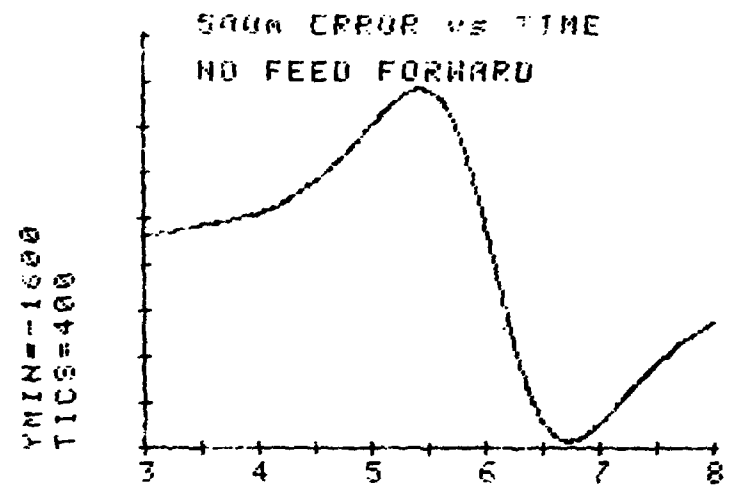

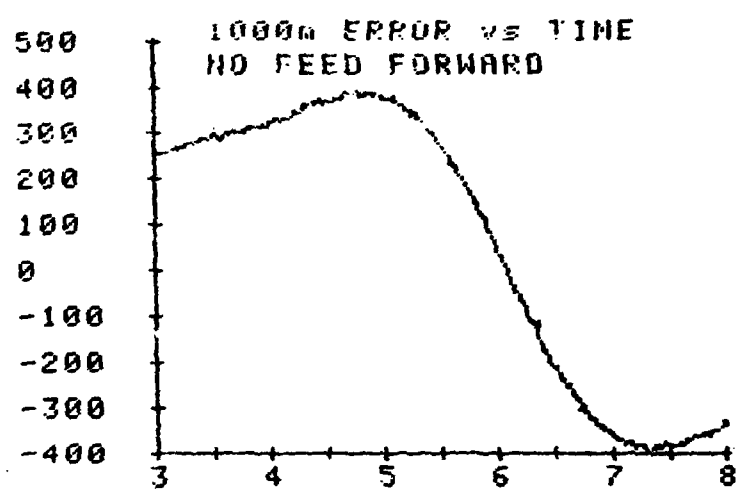

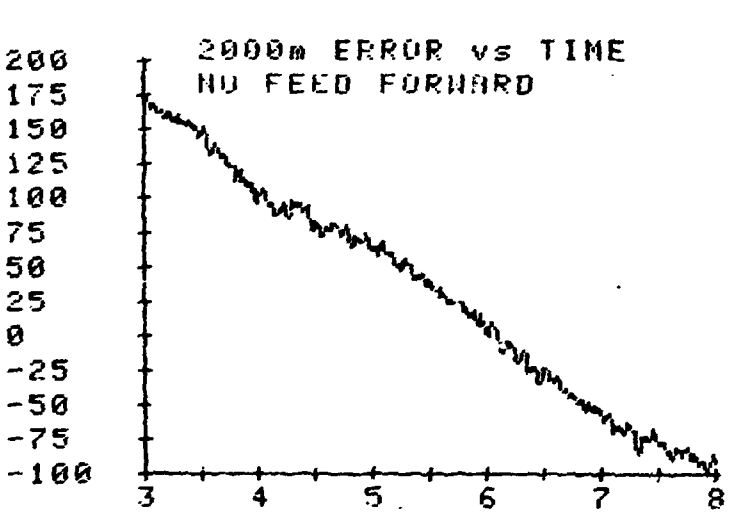

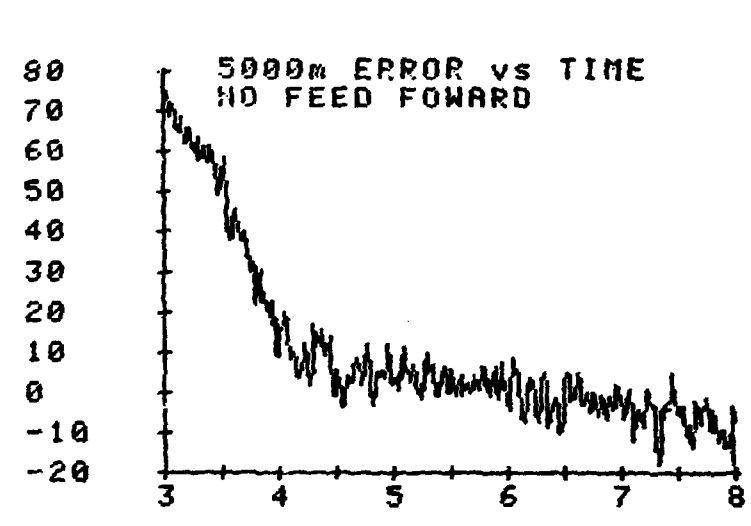

FIGURE 9. BEAM ERRORS FOR NO FEED FORWARD CONFIGURATIONS

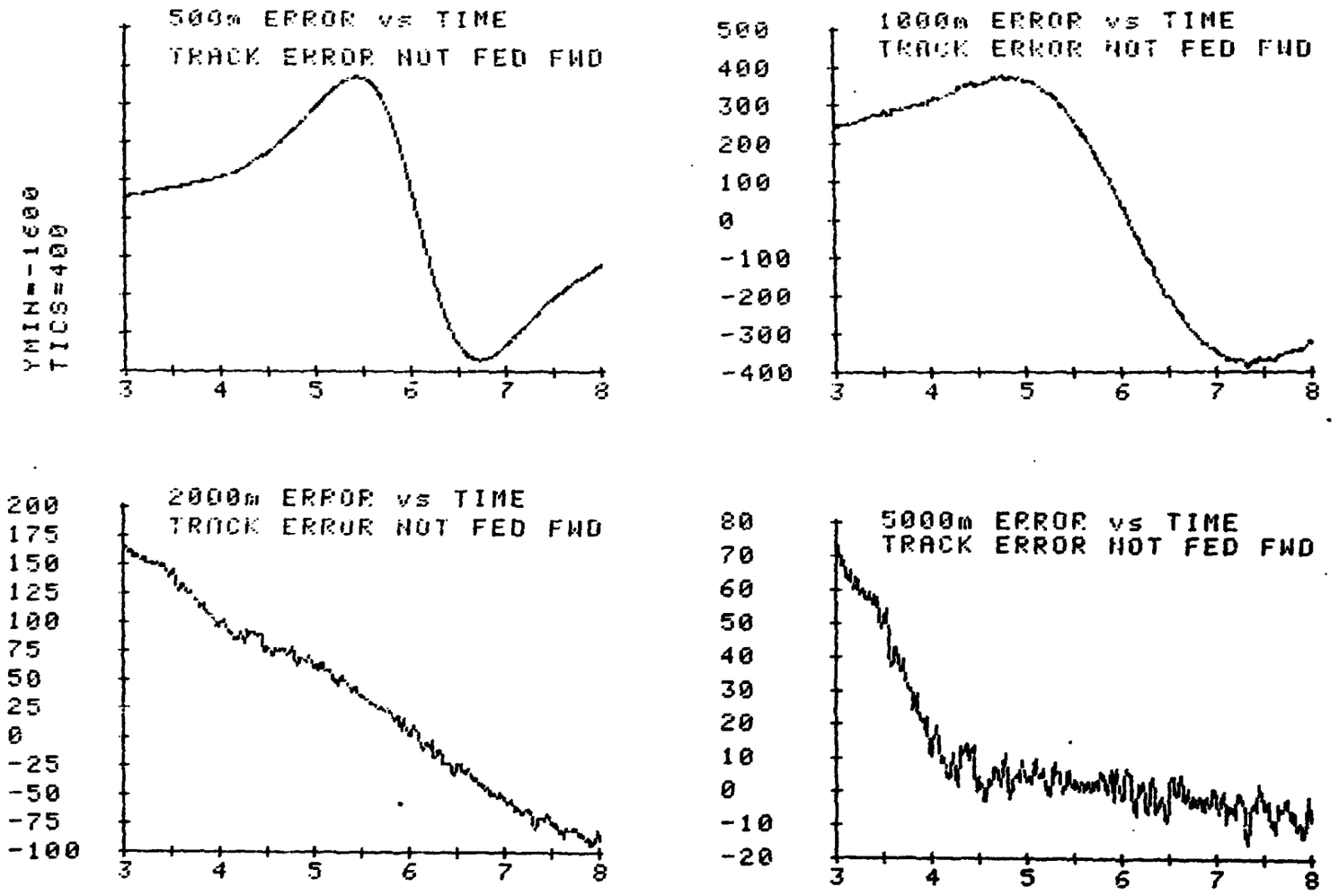

FIGURE 10. BEAM ERRORS FOR TRACKER ERROR NOT FED FORWARD CONFIGURATION

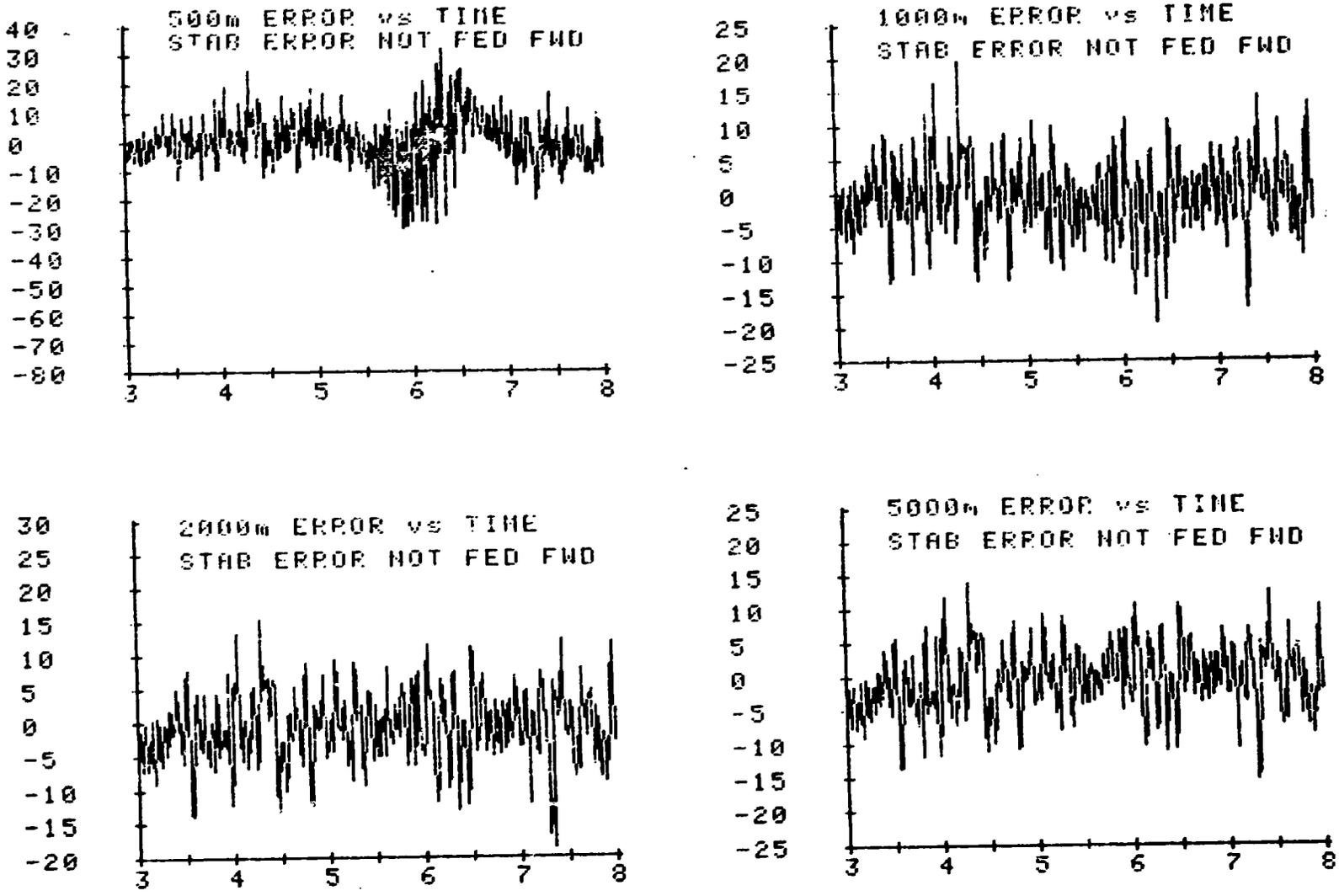

FIGURE 11. BEAM ERRORS FOR STAB ERROR NOT FED FORWARD CONFIGURATION

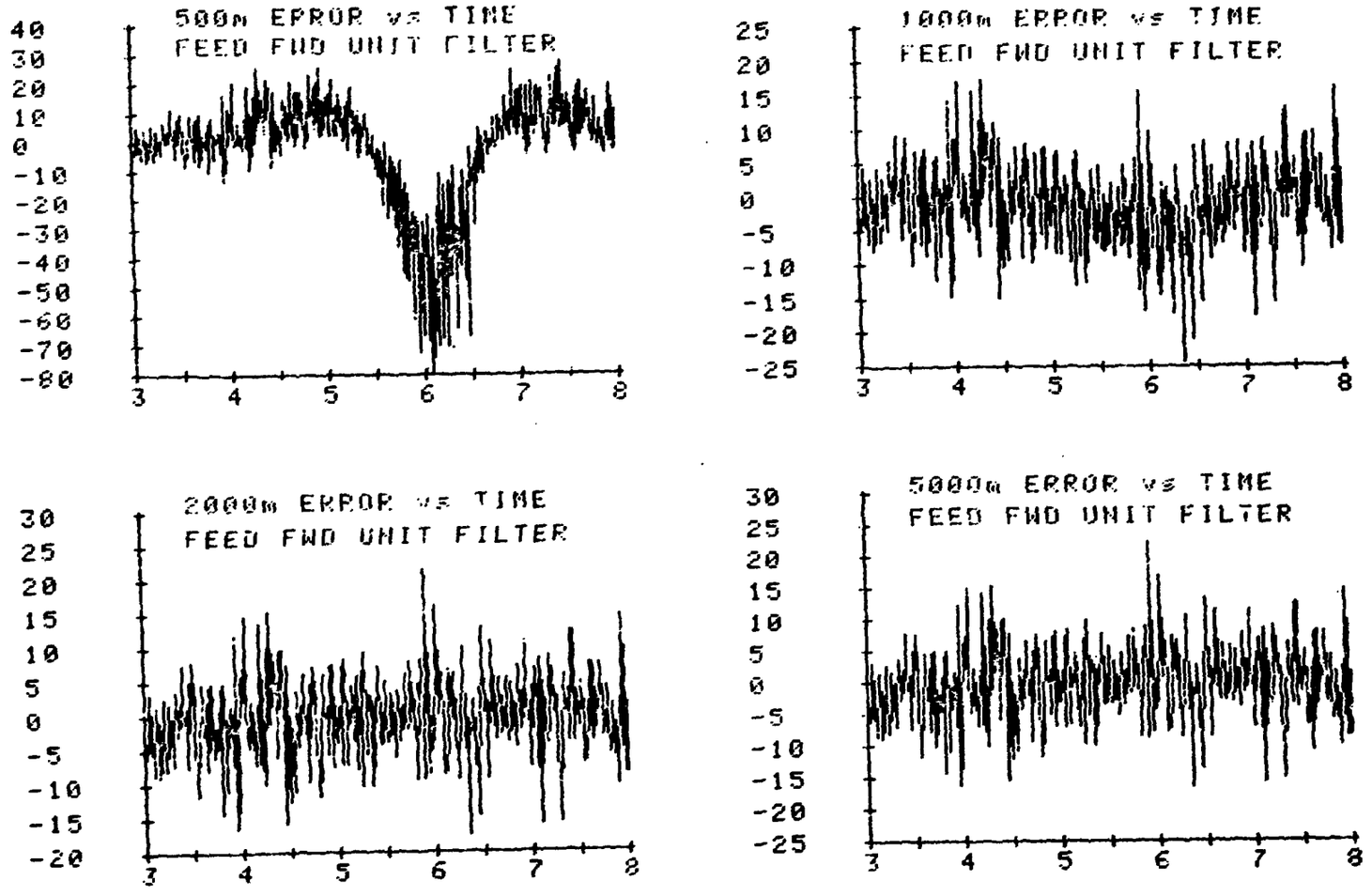

FIGURE 12. BEAM ERROR FOR UNITY FILTER CONFIGURATION

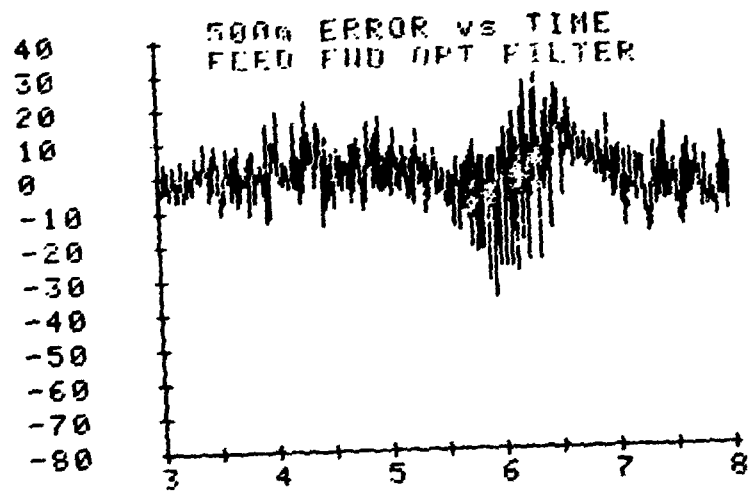

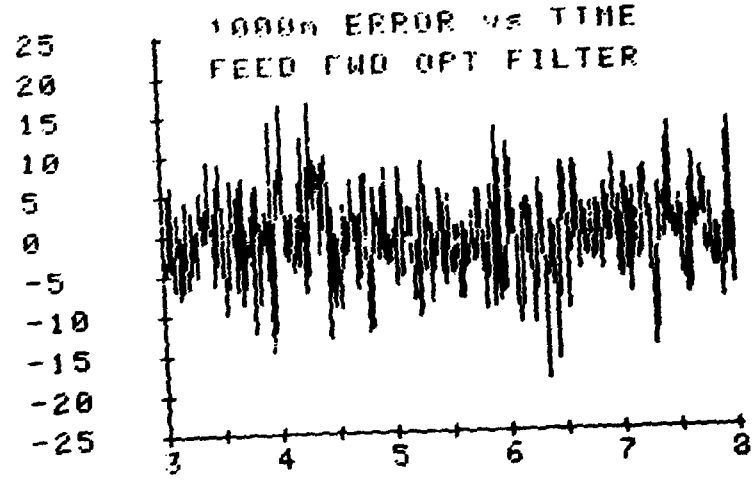

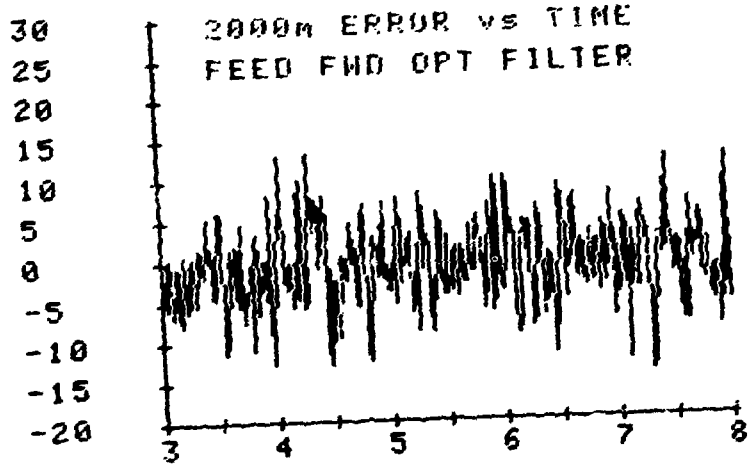

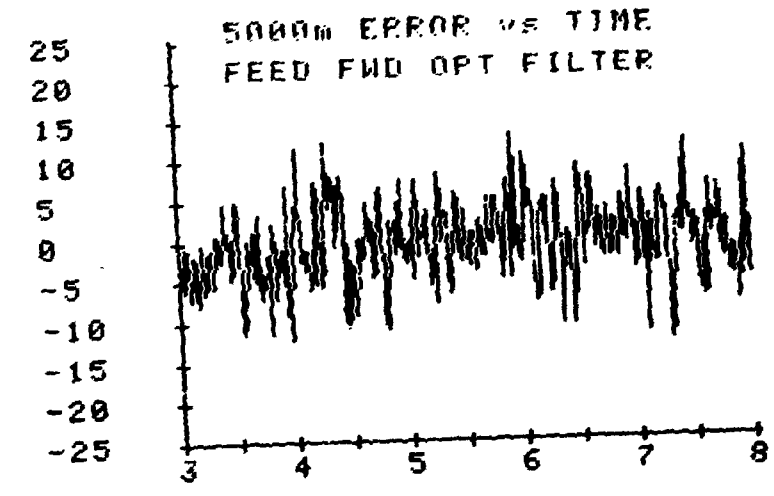

FIGURE 13. BEAM ERROR FOR OPTIMAL FILTER CONFIGURATION

the beam error in μrad versus time in seconds for the 3 to 8 second range. This time range is selected because the main interest is the tracking ability of the APT/AAS of the actual target signal, not of the spline.

In Figures 9 and 10, large beam angle errors (greater than ±50 μrad) occur for the 500m, 1000m and 2000m cases. This is caused by the target having significant relative motion to the APT/AAS (both velocity and acceleration). For the 500m and 1000m cases, the errors drastically increase before and after the time of closest approach by the target (t=6s). This is attributed to the target angle having large angular accelerations before and after t=6s. On the other hand, the 2000m and 5000m cases show the errors tending to montonically decrease. Contrary to the 500m and 1000m cases these also show the randomness due to BMD and tracker noise. Of course this is because the first two cases are dominated by target motion errors, which are many times greater than errors due to the tracker or BMD.

It should also be noted that for the 5000m case the error abruptly decreases just prior to t=4s. This is due to the spline generating a large fictitious acceleration prior to the initiation of tracking. In fact for the 5000m case the APT/AAS exhibits fair tracking capabilities for the no feed forward and tracker error not feed forward configurations, in particular, the errors range between ±20 μrad. For the other cases of these configurations the errors are, in general, too large.

In Figures 11-13, the results from simulating the different cases of the stab error not feed forward, unity feed forward and optimal filter feed forward configurations are summarized. In comparing the corresponding cases of any of these configurations to those of Figures 9-10, it is easily seen that the tracking capabilities have been definitely augmented. Of course the commonality of these three configurations is that all feed the tracker error signal to the AAS in some form.

Both the optimal filter and stab error not fed forward cases feed the tracker error signal to the AAS through the optimal filters designed in [3]. Both of these cases provide less beam error in all four cases of the flyby type scenario than the unity filter case. This was expected since the optimal filter tends to compensate for the tracker not being perfect (continuous output with a unity transfer function).

The stab error not fed forward and the optimal filter configurations are about equal in performances for the 500m and 1000m cases. This is becuase the target signal dominates in these cases. On the other hand for the 2000m and 5000m cases the optimal filter configuration shows a slight increase in tracking performance, than the stab error not fed forward configuration. Such a conclusion is reached by noting that the random "spikes" of the optimal filter configuration are less in magnitude than for the stab error not feed forward configuration. The reason for this increase in performance is that BMD plays a larger role in the beam error for these cases and the stab error is fed forward as part of the scheme to minimize the effects of BMD on the beam error.

In order to determine how the power of the error signal is distributed with respect to frequency the power spectrum density of each of the signals shown in Figures 9-13 were generated using an HP-85 desktop computer and the standard Waveform Analysis Pac purchased from HP [Ref. 5]. The PSD of each error signal is shown in Figures 14-18. The frequency range in each case is 0-50 Hz. It should be noted that the ordinate axis is in decibels/Hz but has been normalized as indicated.

For the Figures 14-15, it is seen that most of the power occurs in the low frequency range. This is caused by the fact that the tracker error is not fed to the AAS in any of these cases, and, hence, the capability of the system to track a moving target is limited.

On the other hand in Figures 16-18, it is seen that the error power is more evenly spread across the spectrum and tends to roll-off on the high frequency end. This was expected since it is known that the PSD's of the BMD tracker error and target signal roll-off at the higher frequencies.

In closely scrutinizing Figures 16-18, only in the 500m cases is any resonance effects detected. A clear resonance is seen to occur at about 40 Hz (about 204.8 on the normalized frequency scale of Figures 16-18). This is attributed to the target having enough motion that natural resonances of the stabilized platform on which the telescope is mounted are excited and, hence contributed significantly to the beam error.

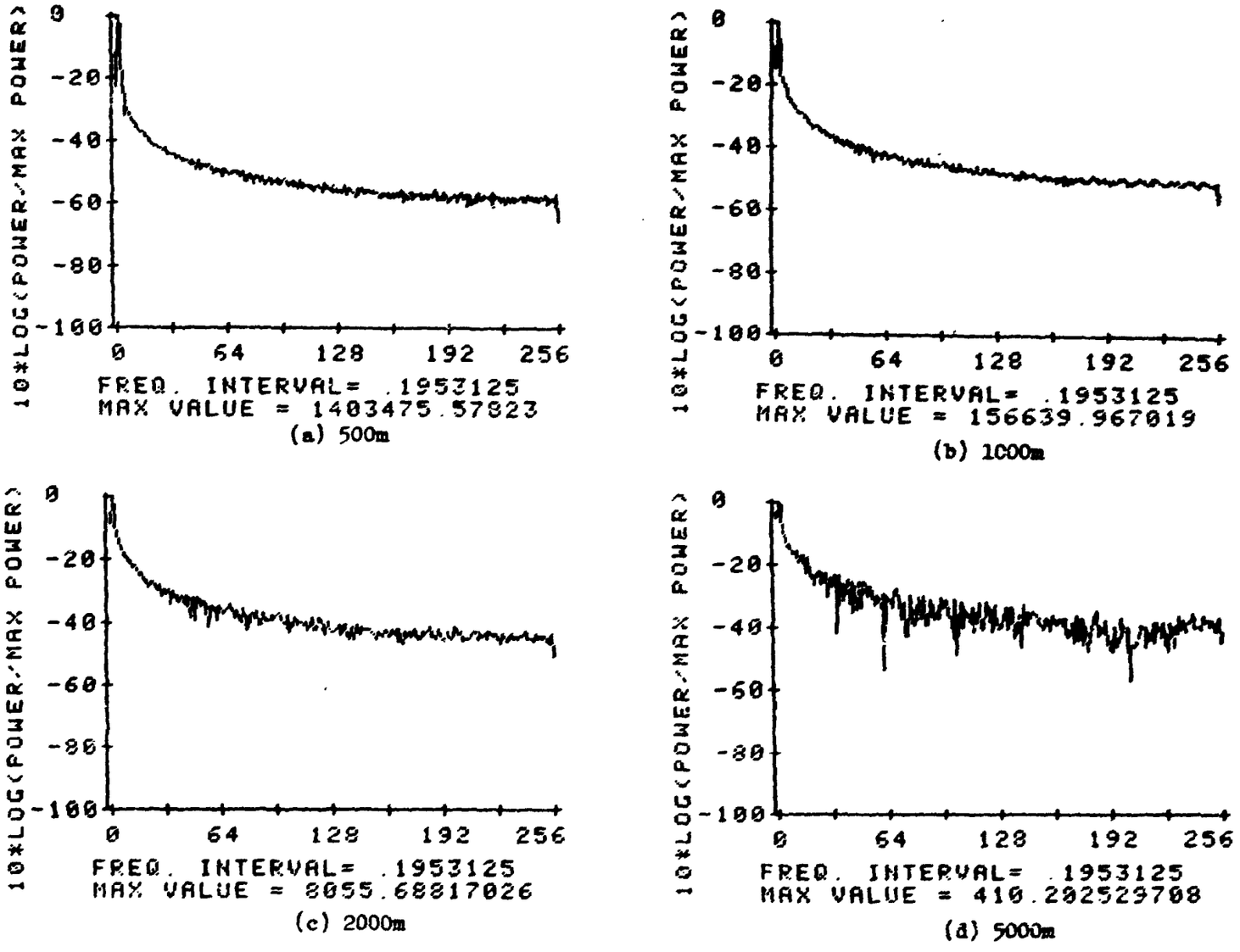

FIGURE 14. PSD OF BEAM ERROR FOR NO FEED FORWARD CONFIGURATION

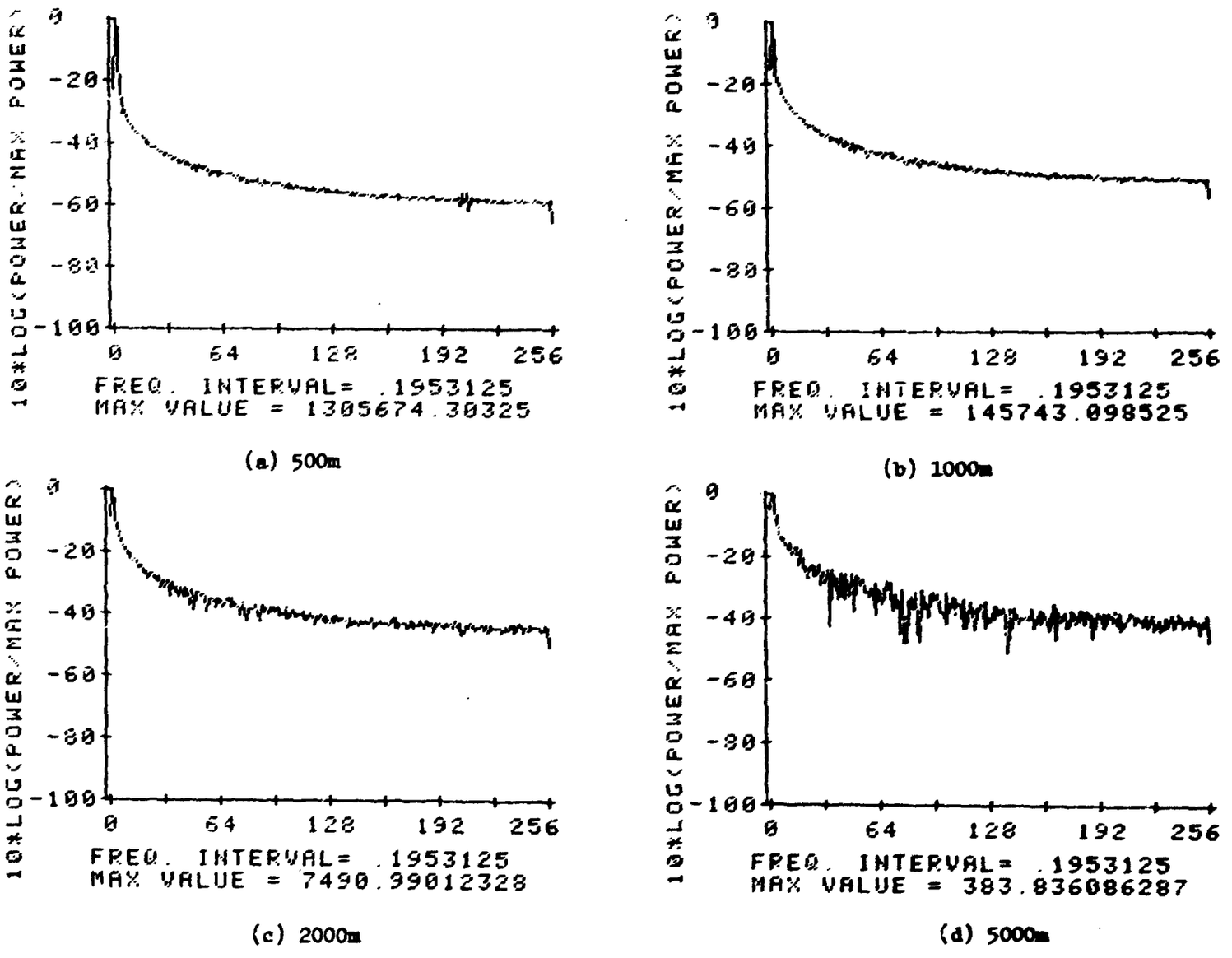

FIGURE 15. PSD OF BEAM ERROR FOR TRACK ERROR NOT FED FORWARD CONFIGURATION

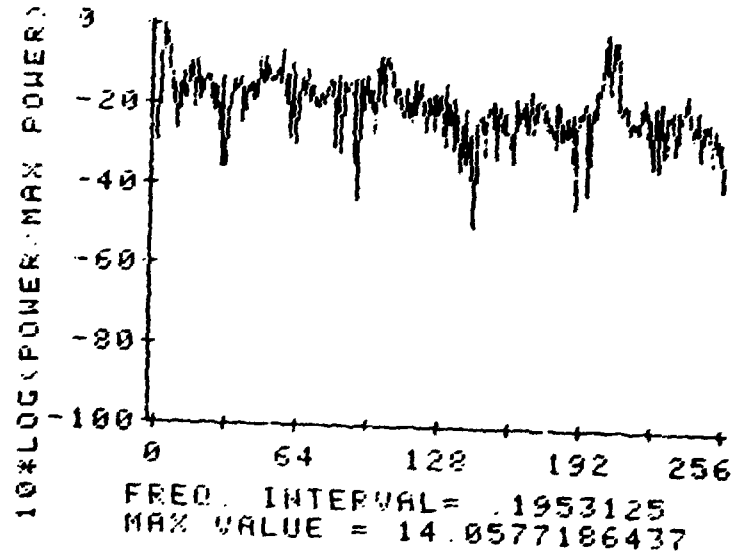

(a) 500m

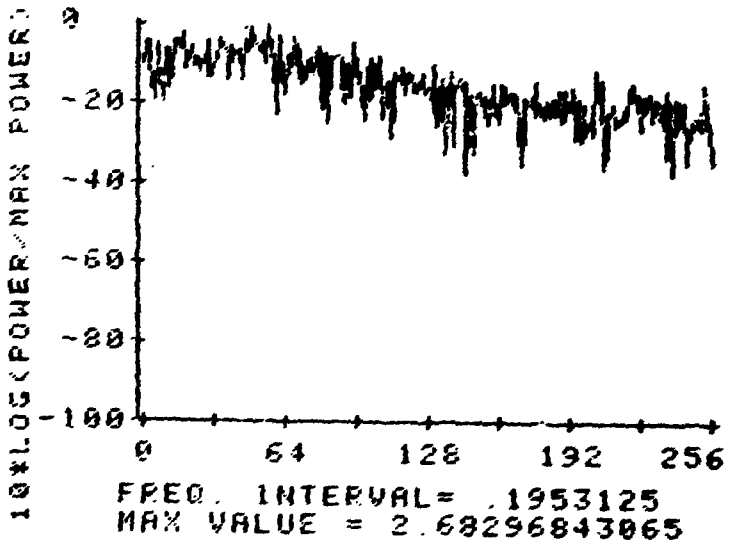

(b) 1000m

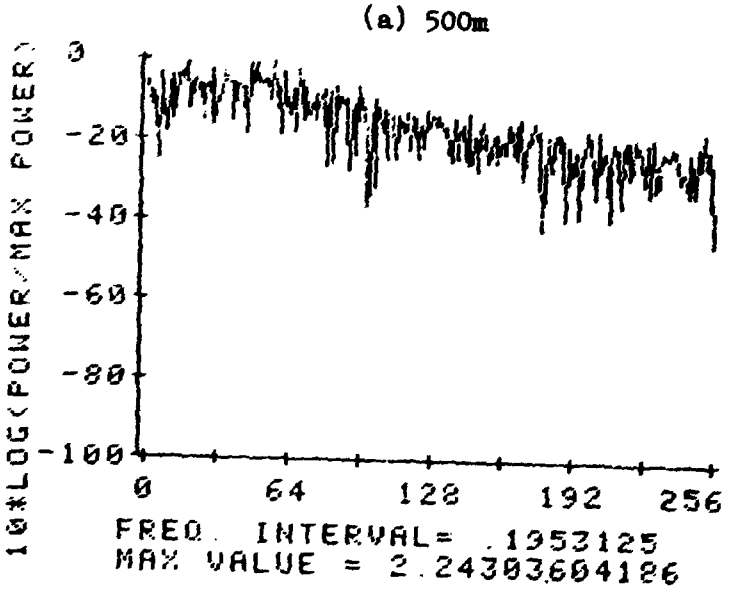

(c) 2000m

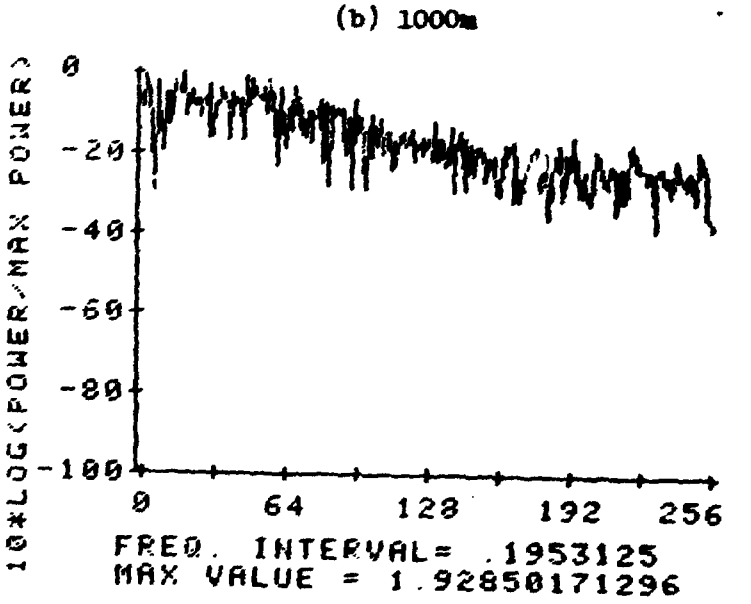

(d) 5000m

FIGURE 16. PSD OF BEAM ERROR FOR STAB ERROR NOT FED FORWARD CONFIGURATION

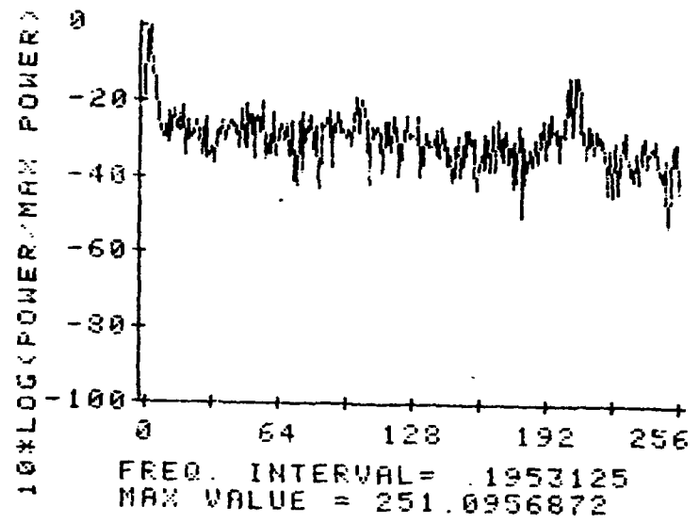

(a) 500m

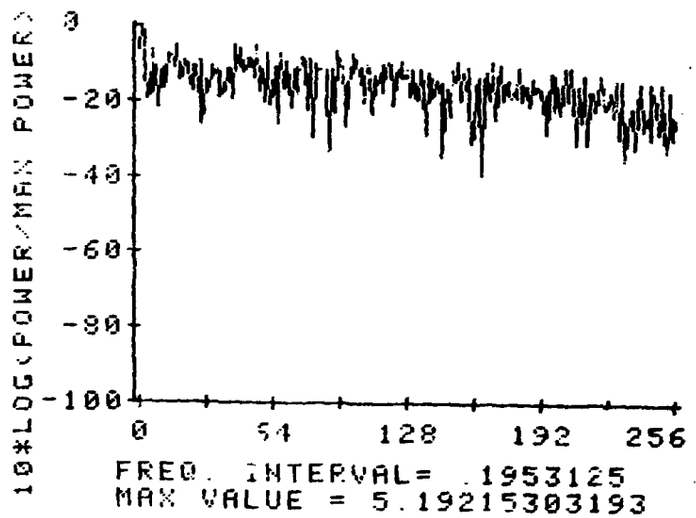

(b) 1000m

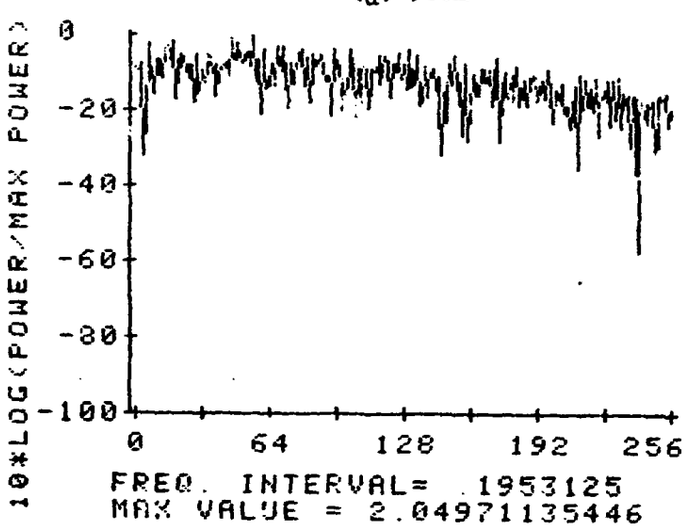

(c) 2000m

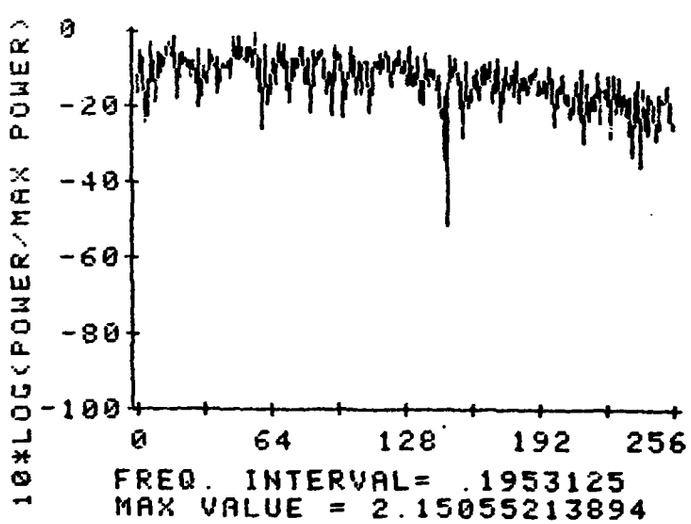

(d) 5000m

FIGURE 17. PSD OF BEAM ERROR FOR UNITY FILTER CONFIGURATION

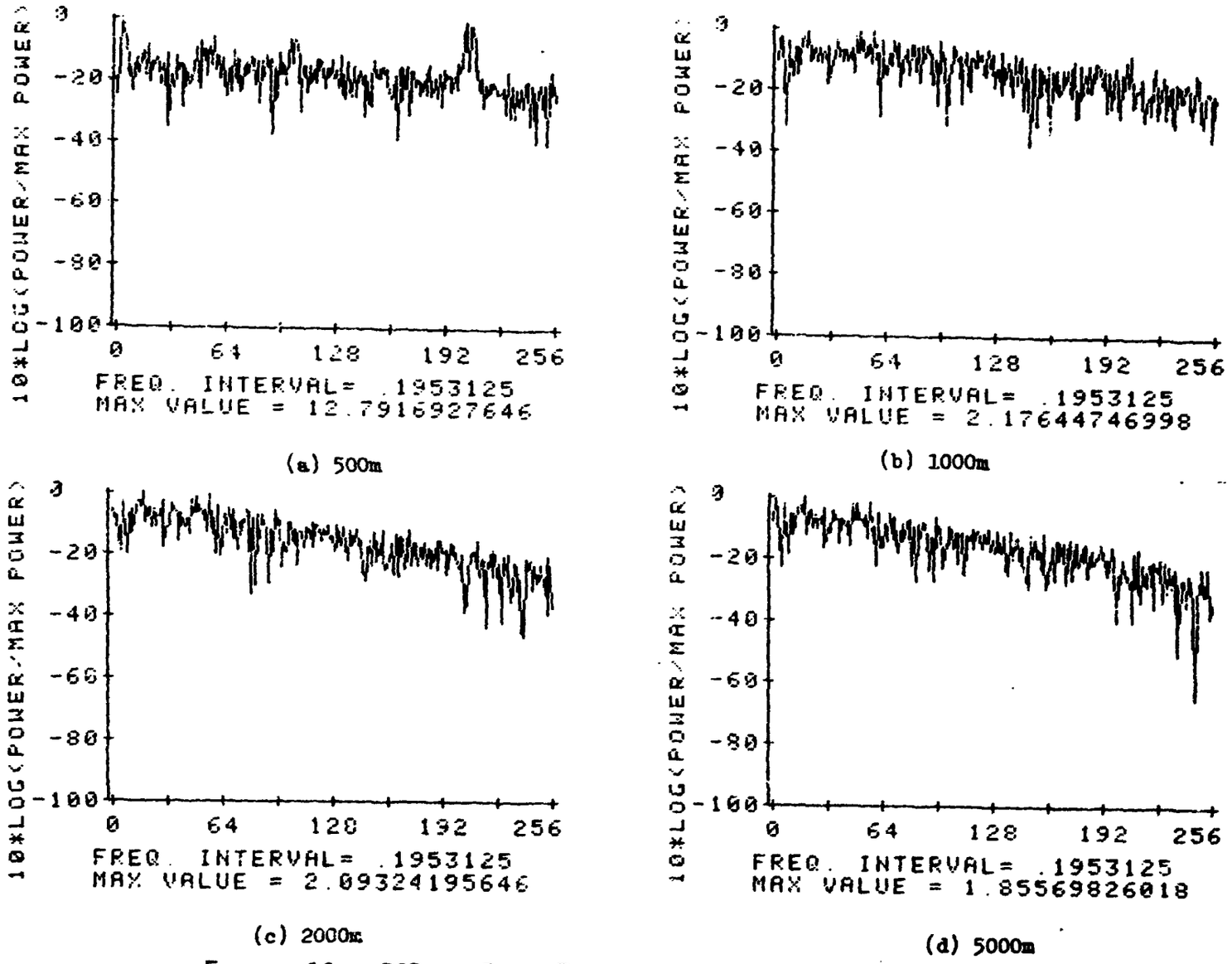

FIGURE 18. PSD OF BEAM ERROR FOR OPTIMAL FILTER CONFIGURATION

The Figures also verify that the configurations where the optimal filters (Figure 16 and 18) were used, produced less beam error than the unity filter configuration (Figure 17). One measure of this is gained by comparing the maximum values of the corresponding cases. By similar comparisons it is seen that the optimal filter configuration with the stab error fed to the IMC and to the AAS (Figure 18) is slightly superior to the stab error not feed forward case (Figure 16).

Figures 9-18 show that much can be gained from the feed forward scheme. A main question is whether the optimal filter schemes produce enough improvement in order to justify the additional electronics. As was pointed out in [3] and earlier in this report, the logical choice for P(s) is unity if an optimal P(s) is not used. In order to provide a clear comparison of the unity filter and optimal filter configurations for each case of the flyby type scenario the PSD's of each were numerically integrated backward starting at 50 Hz.* The corresponding cases are shown in Figures 19-20, where the ordinate values have been scaled by 10^{-12}. In interpretating each plot an ordinate value gives the total amount of power in all frequencies greater than to the corresponding frequency (up to 50 Hz.), and the difference in any two ordinate values gives the power for the corresponding frequency range.

---

*Very little power is contained in the spectrum for frequencies greater than 50 Hz.

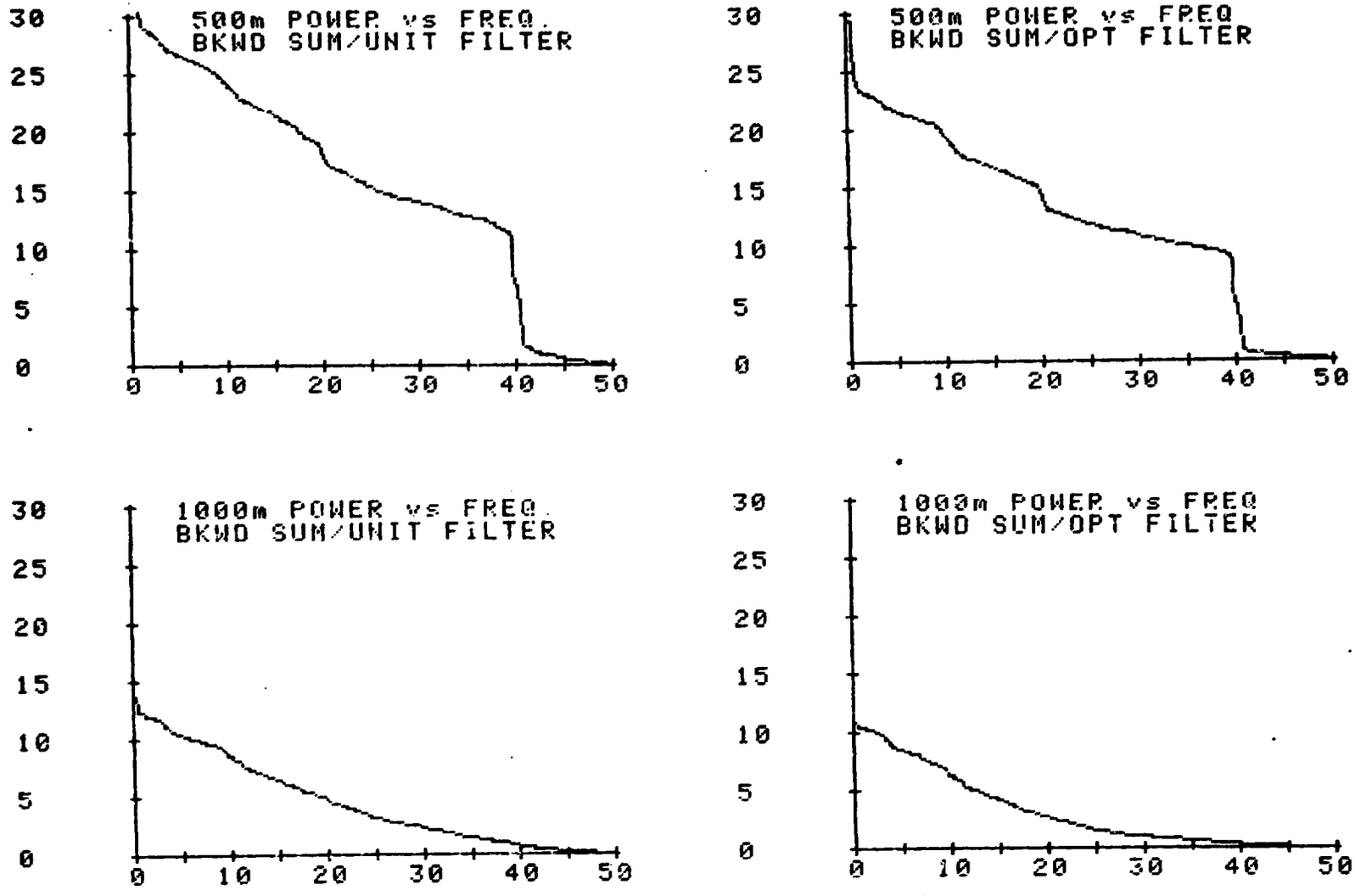

FIGURE 19. BACKWARD SUM OF UNITY FEED FORWARD/OPTIMAL CONFIGURATIONS

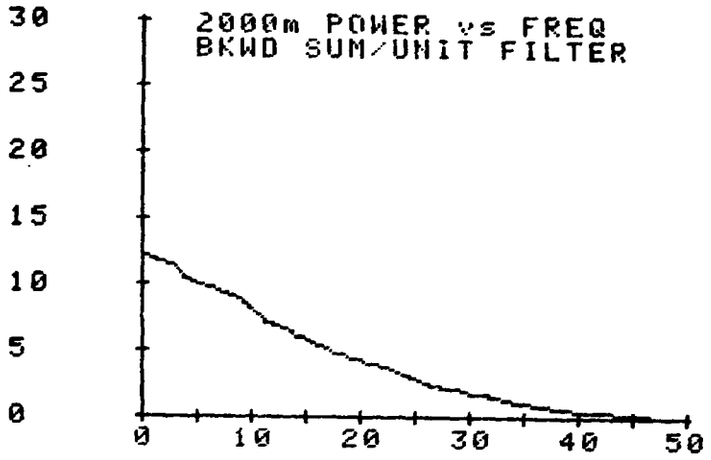

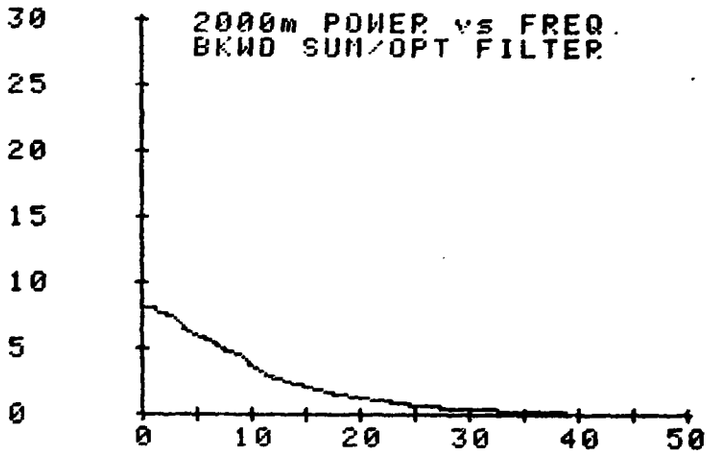

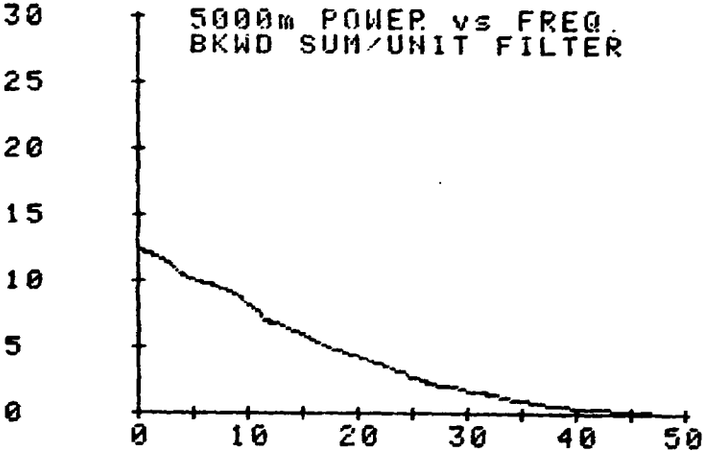

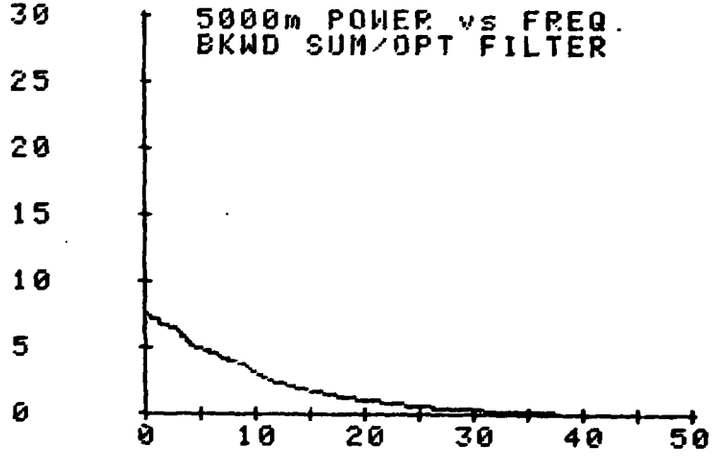

FIGURE 19. (CONTINUED) BACKWARD SUM OF UNITY FEED FORWARD/ OPTIMAL CONFIGURATIONS

If a point by point comparison of corresponding cases is done, it is easily seen that the optimal filter configuration cases are in every instance below the unity filter configuration cases. This verifies that the optimal filters do reduce the error signals.

It should also be noted that the backward sum plots definitely verify that a resonance mode of the system was excited in the 500m case. This is seen by a sharp rise in the backward sum curves at about 40 Hz for the 500m cases. In addition the backward sum curves also show the possibility of another resonance being excited at about 19 Hz for the 500m case. Apparently in none of the other cases were these resonances excited enough to contribute significantly to the beam error.

The backward sum plots can also be used to obtain RMS errors for the beam angle. Since these are a backward integration of two-sided PSD's then

$$\text{RMS ERROR} = \sqrt{2 \times \text{ORDINATE AXIS INTERCEPT}}$$

For the cases at hand the RMS errors are shown in Table II. Again this shows that the optimal filter can definitely improve tracking performance. Furthermore, it should be noted that the RMS values in Table II are comparable to those obtained in [3]. Actually the RMS values are slightly higher than those obtained in [3]. This is expected since the sampling effects of the tracker are included in this study and models of tracker noise and BMD that covered a wider spectrum are used.

Y_0	UNITY FILTER RMS ERROR μrad	OPTIMAL FILTER RMS ERROR μrad
500m	8.94	7.62
1000m	5.10	4.69
2000m	4.96	4.00
5000m	4.96	3.87

TABLE II: COMPARISON OF RMS ERRORS FOR UNITY FILTER vs OPTIMAL FILTER CONFIGURATIONS

V. CONCLUSION AND RECOMMENDATIONS

A feed forward scheme for controlling the LOS of a high energy laser beam was devised for reducing errors of the beam angle due to BMD and for tracking targets with significant motion. As was shown in [1] and [2] the capability of the system to reject BMD was greatly enhanced by this scheme, but the effects on beam error due to tracker noise was amplified. A third study [3] was initiated to design a compromising filter that would provide the capabilities to satisfactorily reject BMD and tracker noise signals and to track targets with significant motion. This was accomplished by designing a filter to minimize the RMS error of the beam angle.

However, the study in [3] used RMS values and simplifying assumptions in regard to the system, e.g., the sampling effects of the tracker were neglected. Since the results produced by [3] appeared very promising it was decided that follow-on studies should be initiated. In particular, it was decided that time domain studies should be conducted to verify the previous frequency domain studies.

These time studies are summarized in this report. In accomplishing them some of the simplifying assumptions made in [3] were removed, e.g., the sampling effects of the tracker were included. The results contained in this report closely agree with those contained in [3]. As a general rule the RMS beam angle errors are slightly greater, but this was expected since more

exact models and signals were used. As a result of the studies in [1], [2], [3], and this repo t the feed forward scheme appears to be very promising for beam control.

There are several follow-on studies that should be conducted. Among these are

(1) The scheme has been tested with an ideal flyby type scenario. It should be tested with typical scenarios.

(2) The study in [3] produces different filters for each case of the flyby type scenario. These designs should be repeated for other scenarios, and it should be determined if a pattern exists for determining the filter coefficients for a general type scenario. It might very well turn out that an adaptive filter could be used, i.e. based upon target motion the system should automatically update the coefficients of the filter.

(3) More accurate models of the system signals and components should be used in the design of the optimal filters.

In accomplishing any or all of the above suggested studies the code developed in [3] (or a modified version) could be used. Of course each of the suggested frequency domain studies should be paralleled with time domain studies to verify that the system is operating within its designed dynamical range.

REFERENCES

1. R. L. Van Allen, "Simulation Study of a Track Error/Stab Error Feed Forward Correction for Cycle IV," MEMO FOR RECORD, Air Force Weapons Laboratory, Kirtland AFB, NM, October 1978.

2. R. L. Van Allen, "Track Error/Stab Error Feed Forward Con'd," MEMO FOR RECORD, Air Force Weapons Laboratory, Kirtland AFB, NM, December 1978.

3. J. R. Mitchell, "Optimization of the Feed Forward Technique for Beam Control in the APT, "Final Report for the 1979 USAF-SCEEE Summer Faculty Research Program, Air Force Office of Scientific Research, Contract No. F49620-79-0038, Bolling AFB, D.C. 20332, August 1979.

4. H. E. Petersen and F. J. Sansom, "MIMIC - A Digital Simulator Program," Wright Patterson AFB, CH, May 1965.

5. "HP-85 Waveform Analysis Pac," Hewlett Packard, 100 N.E. Circle Blvd., Corvallis, OR 97330, February 1980.

APPENDIX

The following is a listing of the APT/AAS MIMIC Simulation with corresponding data for the 500m case. Definitions of several of the pertinent constants and parameters used in the code are as follows:

SPD - Sampling period of tracker

SPD2 - Sampling period used for generating BMD

V - Target Velocity (m/s)

YO - Minimum Approach distance s(m)

TDL - Tracker Delay (s)

LCV12, LCV13, & LCV14 - Logical Control Variables for Determining the Control Configuration (1. - True, 0. - False)

A11, A12, B11, and B12 - Numerator Coefficients of Optimal Filter

A21, A22, B21, and B22 - Denominator Coefficients of Optimal Filter

```
C
C                          SIMULATION OF THE BEAM CONTROL SYSTEM USING
C                          BOTH THE APT AND AAS TO FORM VARIOUS FEEDFORWARD
 SCHEMES
C
C
                     CON(TZ,SPD,TBMD,SPD2)
                     CON(C1,T1,C2,T2,C3,C4)
                     CON(VAR1,NUM1,VAR2,NUM2)
                     CON(SIGNAL,TRKERR,BMD)
                     CON(DT,DTMAX,DTMIN,PERIOD,TMAX)
                     CON(V,Y0)
                     CON(A3,A2,A1,A0)
                     CON(P1,P2,P3,P4,P5,P6)
                     CON(P7,P8,P9,P10,P11,P12)
                     CON(TDL,TDX,X1)
                     CON(X4,X66,X6)
                     CON(LCV12,LCV13,LCV14)
                     PAR(A11,A12,B11,B12)
                     PAR(A21,A22,B21,B22)
C
C
C         IF LCV12=TRUE,THEN THE TRACK ERROR IS FED FORWARD.
C
C         IF LCV12=FALSE,THEN THE TRACK ERROR IS NOT FED FORWARD.
C
C         IF LCV13=TRUE,THEN THE STAB ERROR IS FED TO THE AAS.
C
C         IF LCV13=FALSE,THEN THE STAB ERROR IS NOT FED TO THE AAS.
C
C         IF LCV12 AND LCV13 ARE TRUE,THE COMPLETE FEEDFORWARD
C         SCHEME IS IMPLEMENTED.
C
C         IF LCV12 AND LCV13 ARE FALSE,THE BEAM IS CONTROLED BY THE APT O
NLY.
C
C         IF LCV14=TRUE,THEN THE UNITY TRACK ERROR FEEDFORWARD
C         FILTER IS IMPLEMENTED.
C
C
GENERATION OF TARGET SIGNAL
           TX        T-6.
           LCV1      FSW(T,TRUE,TRUE,FALSE)
           LCV2      FSW(T-4.,TRUE,TRUE,FALSE)
           LCV3      NOT(LCV2)
           LCV4      FSW(T-8.,TRUE,TRUE,FALSE)
           LCV5      AND(LCV3,LCV4)
           LCV6      NOT(LCV4)
           LCV7      FSW(T-TMAX,FALSE,FALSE,TRUE)
 LCV13     P11       1.0
 LCV1      CON1      324.*A3-72.*A2+18.*A1-6.*A0
 LCV1      CON2      -4.*A3+8.*A2/3.-2.*A1+2.*A0
 LCV1      CON3      2.*V/Y0
```

```
 LCV1     XP2       V*2.
 LCV1     MIT       -2.
 LCV1     XM2       V*MIT
 LCV1     CON5      (((+A3/4.*MIT+A2/3.)*MIT+A1/2.)*MIT+A0)*MIT-CON1
 LCV1     CON6      ATN(XM2/Y0)
 LCV3     X         V*TX
 LCV5     THETA     ATN(X/Y0)-CON6+CON5
 LCV2     PART1     (((+A3/4.0*TX+A2/3.0)*TX+A1/2.0)*TX+A0)*TX-CON1
 LCV1     CON4      ATN(XP2/Y0)-CON6+CON5-CON2
 LCV6     PART2     (((-A3/4.0*TX+A2/3.0)*TX-A1/2.0)*TX+A0)*TX+CON4
          SIG1      LSW(LCV2,PART1,0.)
          SIG2      LSW(LCV5,THETA,0.)
          SIG3      LSW(LCV6,PART2,0.)
          SIGNAL    SIG1+SIG2+SIG3
GENERATION OF BMD
          LCV10     FSW(T-TBMD,FALSE,TRUE,TRUE)
 LCV10    BMDI      C2*RNG(0.,VAR2,NUM2)
 LCV10    TBMD      TBMD+SPD2
          BMD2      INT(BMDI,0.0)
          BMD3      C4*FTR(BMDI,T2)
          BMD       C3*(BMD2+BMD3)
          IBMD      INT(BMD,0.)
          ISBMD     INT(BMD*BMD,0.)
TRACKER ERROR SIGNAL
          LCV9      FSW(T-TZ,FALSE,TRUE,TRUE)
 LCV9     TRKERR    C1*RNG(0.,VAR1,NUM1)
 LCV9     TZ        TZ+SPD
          INTRER    INT(TRKERR,0.)
          INSQTE    INT(TRKERR*TRKERR,0.)
          SIG       ZOH(SIGNAL,SPD)
 LCV12    X66       ZOH(X6,SPD)
          GANG1     ZOH(GANG,SPD)
OUTPUT OF HOLD DEVICE
          X11       SIG+TRKERR-P11*X66-GANG1
OUTPUT OF DELAY
          LCV11     FSW(T-TDX,FALSE,TRUE,TRUE)
 LCV11    TDX       TDX+SPD
 LCV11    X1        X11
OUTPUT OF TRACK LOOP COMPENSATOR
          X2        33.02*X1+350.0*INT(X1,0.0)
STABILIZE PLATFORM ERROR SIGNAL
          ESTAB     INT(X2-X3,0.0)
PLATFORM SIGNAL
          X3        BMD+W1
PLATFORM DYNAMICS
          W1        INT(W2,0.0)
          W2        INT(W3,0.0)
          W3        INT(P1*W3+P2*W2+P3*W1+P10*Z1,0.0)
          Z1        P4*ESTAB+P5*INT(ESTAB,0.0)
GIMBAL ANGLE
          GANG      INT(X3,0.0)
```

```
OPTIMAL FILTER TRANSFER FUNCTION
          LCV16     NOT(LCV14)
          LCV15     AND(LCV12,LCV16)
 LCV14    X4        X1
 LCV15    X41       X1*A11/B11+FTR((A12/B12-A11/B11)*X1,B11/B12)
 LCV15    X4        X41*A21/B21+FTR((A22/B22-A21/B21)*X41,B21/B22)
100 HZ STAB FILTER
 LCV13    X6        FTR(ESTAB,F12)
AUTO ALIGNMENT SYSTEM ERROR
          EAAS      X4+P11*X6-X5
AUTO-ALIGNMENT SYSTEM DYNAMICS
          X51       P6*EAAS+P7*INT(EAAS,0.0)
          X5        INT(X51,0.0)
BEAM ANGLE
          BANG      X5+GANG
ERROR BETWEEN BEAM ANGLE AND TARGET SIGNAL
          ERROR     SIGNAL-BANG
ROOT MEAN SQUARE VALUE OF ERROR
          MSE       INT(ERROR*ERROR/PERIOD,0.0)
                    HDR(TIME,SIGNAL,GIMBAL,BEAM,ERROR,MSE)
                    HDR( , ,ANGLE,ANGLE)
                    HDR
                    HDR( ,I.TRK,IS.TRK,I.BMD,IS.BMD)
                    HDR
                    OUT(T,SIGNAL,GANG,BANG,ERROR,MSE)
                    OUT( ,INTRER,INSQTE,IBMD,ISBMD)
                    OUT
                    FIN(T,TMAX)
                    END
 0.          .01666666666 0.          6.28319 E-03
2.192   E-06 2.652  E-03 -1.0        .005          9.403  E-04 .1061
2.0          3975319.      2.0          1234567.
1.0          0.0          0.0
.01           3.0     E-03 1.0E   E-05 8.0          8.0
457.2        5000.0
-2.586056E-3-3.067474E-2-8.880281E-21.288565E-02
-279.624     -369514.11   -78369905.0  265.3       10000.0      1987.
1.248   E 06.0045475     -352692.0    78369905.    0.0              1.592E-03
.003          .003          0.0
0.0          0.0          0.0
0.0          0.0          0.0
1.3745       7.9788       1.6585       10.0
1.1542       100.09       2.6441       80.0
                    ENDATA
                    STOP
EOF:149 SCAN:44
```

```
OPTIMAL FILTER TRANSFER FUNCTION
          LCV16     NOT(LCV14)
          LCV15     AND(LCV12,LCV16)
 LCV14    X4        X1
 LCV15    X41       X1*A11/B11+FTR((A12/B12-A11/B11)*X1,B11/B12)
 LCV15    X4        X41*A21/B21+FTR((A22/B22-A21/B21)*X41,B21/B22)
100 HZ STAB FILTER
 LCV13    X6        FTR(ESTAB,P12)
AUTO ALIGNMENT SYSTEM ERROR
          EAAS      X4+P11*X6-X5
AUTO-ALIGNMENT SYSTEM DYNAMICS
          X51       P6*EAAS+P7*INT(EAAS,0.0)
          X5        INT(X51,0.0)
BEAM ANGLE
          BANG      X5+GANG
ERROR BETWEEN BEAM ANGLE AND TARGET SIGNAL
          ERROR     SIGNAL-BANG
ROOT MEAN SQUARE VALUE OF ERROR
          MSE       INT(ERROR*ERROR/PERIOD,0.0)
                    HDR(TIME,SIGNAL,GIMBAL,BEAM,ERROR,MSE)
                    HDR( , ,ANGLE,ANGLE)
                    HDR
                    HDR( ,I.TRK,IS.TRK,I.BMD,IS.BMD)
                    HDR
                    OUT(T,SIGNAL,GANG,BANG,ERROR,MSE)
                    OUT( ,INTRER,INSQTE,IBMD,ISBMD)
                    OUT
                    FIN(T,TMAX)
                    END
 0.          .01666666666 0.          6.28319 E-03
2.192   E-06 2.652  E-03 -1.0        .005          9.403  E-04 .1061
2.0          3975319.      2.0          1234567.
1.0          0.0          0.0
.01           3.0     E-03 1.0E   E-05 8.0          8.0
457.2        5000.0
-2.586056E-3-3.067474E-2-8.880281E-21.288565E-02
-279.624     -369514.11   -78369905.0  265.3       10000.0      1987.
1.248   E 06.0045475     -352692.0    78369905.    0.0             1.592E-03
.003          .003          0.0
0.0          0.0          0.0
0.0          0.0          0.0
1.3745       7.9788       1.6585       10.0
1.1542       100.09       2.6441       80.0
                    ENDATA
                    STOP
EOF:149 SCAN:44
```